

Improving Small-Plantation and Woodlot Inventory

J. P. Dash, M.S. Watt, S. Puliti, A. Gordon, G. Pearse



Date: June 2018
Number: GCFF-T005

Improving Small-Plantation and Woodlot Inventory

Table of contents

Executive Summary	1
Introduction.....	2
Methodology overview.....	3
Theme 1. Testing different sampling strategies for forest inventories using UAV laser scanning and photogrammetric data	4
1. Introduction	4
2. Materials	6
3. Methods	9
4. Results	12
5. Discussion.....	16
References.....	17
Theme 2: A Community Approach – Plot sharing to provide the benefits of large scale to Woodlot growers	19
Background.....	19
Case study.....	21
Conclusion	30
References.....	30
Theme 3: Calibrating a National ALS model of Total Standing Volume using Local Sample Plots	31
Recommendations and Conclusions.....	39
Related articles and communications associated with this project.	40
Acknowledgements	40

Disclaimer

This report has been prepared by New Zealand Forest Research Institute Limited (Scion) for Forest Growers Research Ltd (FGR) subject to the terms and conditions of a research fund agreement dated 1 April 2014.

The opinions and information provided in this report have been provided in good faith and on the basis that every endeavour has been made to be accurate and not misleading and to exercise reasonable care, skill and judgement in providing such opinions and information.

Under the terms of the Services Agreement, Scion's liability to FGR in relation to the services provided to produce this report is limited to the value of those services. Neither Scion nor any of its employees, contractors, agents or other persons acting on its behalf or under its control accept any responsibility to any person or organisation in respect of any information or opinion provided in this report in excess of that amount.

Executive Summary

This research was aimed at exploring and further developing the opportunities provided by modern remote sensing techniques for growers of small-forests and woodlots in New Zealand. These forests represent a significant proportion of the New Zealand plantation estate and are not well served by forest inventory methods using remotely sensed data that have been developed previously. Our approach sought to investigate methods that can help small-forest growers gain access to research developments provided by remote sensing. Three research themes were investigated and delivered new insight into the use of remote sensing for small-plantations and woodlots. In a world first we have developed new statistical estimators and sampling strategies that allow integration of 3D data collected from a UAV to be incorporated into a small sample size framework suitable for use in a common forest measurement scenario. Through a detailed case study we have also made significant strides towards developing optimal sampling and data collection procedures in this context. The results are extremely promising and we have provided new methodologies for the application of these techniques. We have also developed a framework to enable small-forest growers to collaborate, share data, and utilise open access datasets commonly by governmental organisations for non-forestry purposes. A comprehensive case study has shown that this approach is suitable for providing yield estimates for numerous small-forest entities across large areas. Furthermore, this was achieved using only free remotely sensed data and pre-existing field measurements. It is very likely that the case study employed here provides the most accurate yield description for small-forests in the Southern North Island and this method could be extended up to the national level should an appropriate Lidar dataset become available.

Introduction

Small-plantations represent a significant proportion of the New Zealand plantation resource. Growers of these woodlots include an estimated 12,000-14,000 small-forest owners and the majority of this vital resource is found on New Zealand's farms. In total these woodlots constitute approximately 36% of the total NZ plantation estate by area. Within certain areas the small-plantations make up the majority of the available wood supply.

Small-plantations and woodlots are difficult to accurately measure and value in a cost-effective way. The conventional method used for valuation involves installation of sufficient ground based sample plots to estimate total volume and volume of log grades within predefined error limits. Use of this methodology to precisely estimate volume and value is often prohibitively expensive in a small plantation, as compared to large plantations, small plantations typically have high variation relative to their area. As a consequence, insufficient plots are typically installed and measured, with the upper limit sometimes determined by the maximum number of plots an inventory crew can install in a single day (approximately 8). If insufficient plots are installed the resulting estimates of volume and plantation value may have a low level of accuracy and the precision estimates may be misleading. As a consequence log buyers or new owners may undervalue the woodlot to compensate for the high degree of uncertainty around value. Alternatively, growers may overestimate the value of their resource leading to poor realisation of revenue at harvest. This can have detrimental effects on rural businesses and lead to a poor perception of forestry as a viable investment for farming communities. To support the management of small-plantations, and ensure the sustainability of this strategically important wood supply source, it is important to continue to research and improve methods for estimating yields, taking advantage of new technologies where appropriate.

The goal of this project is to research methods for integrating modern, cost-effective, remotely sensed data into forest inventories. These methods will allow for more precise estimates of woodlot volume and value, without resulting in substantial increases in inventory cost. Analyses will be undertaken that quantify the cost of integrating this data and the extent to which the integration improves inventory precision for woodlots. This research is innovative as the application of remotely sensed data and modern statistical techniques to small-plantations and woodlots has received little research focus in New Zealand in recent years.

Objectives

The objectives of this research project were as follows:

- To undertake research that improves forest inventory for small-plantations and woodlots.
- To investigate approaches that make measurement more cost effective.
- To investigate approaches that have the potential to make the benefits of existing remotely sensed data and new statistical methods available to stakeholders. This will include use of existing data in novel or alternative analytical frameworks that can be useful for estimation in small-plantations and woodlots.
- To disseminate the findings to small-plantation and woodlot growers.

Methodology Overview

This project has the following three distinct research themes as described below:

1. Using data from a single small woodlot, theme 1 tested different sampling strategies for reducing error in forest inventories using UAV acquired laser scanning and photogrammetric data. The sampling strategies included model based estimation and hybrid inference which involve, respectively, complete or partial coverage of the stand.
2. Theme 2 investigated the potential benefits to small plantation growers that may result from data sharing. Using a large dataset collected across the southern North Island this theme investigated the utility of a nearest neighbour estimation (k-NN) approach for predicting yield estimates. A key objective was to determine if it is possible for small-plantation growers to collaborate through data sharing and, where available, take advantage of open access datasets to provide yield estimates for small-plantations across an entire region.
3. Theme 3 investigated the feasibility of utilising a national LiDAR based model to predict total stem volume within 10 small woodlots. This was undertaken either through (i) uncalibrated direct prediction of volume using the LiDAR model and (ii) integration of calibrated predictions with plot data using regression estimation. The error was compared between these two approaches and the use of plot data only.

Results from these research themes are summarised in the following sections.

Theme 1. Testing different sampling strategies for forest inventories using UAV laser scanning and photogrammetric data

1. Introduction

The use of unmanned aerial vehicles (UAVs) or systems (UAS) within the civilian market has increased dramatically over the last five years. Within the realm of environmental monitoring UAVs have been used to collect information from light detection and ranging (LiDAR), thermal, multispectral and hyperspectral sensors which are processed to produce either spectral data or three dimensional point clouds (Salamí et al. 2014). Although they are underutilised within plantation forestry, there is considerable potential for use of UAVs within this sector and a number of potential applications have already emerged that include inventory, post-harvest site assessment, characterisation of weed competition, and detection of disease (Wallace et al. 2016; Dash et al. 2017; Watt et al. 2017; Puliti et al. 2017; Puliti et al. 2015; Pierzchała et al. 2014; Puliti et al. 2018b; Talbot et al. 2017; Goodbody et al. 2017).

Rapid growth in the use of UAVs is predicted to continue (Nex and Remondino 2014; Hugenholtz et al. 2012; Watts et al. 2012) as they offer greater operational flexibility compared to other platforms and can collect data under a variety of atmospheric conditions (Whitehead and Hugenholtz 2014). Among available aerial platforms, UAVs provide an unparalleled resolution and data density. Spectral imagery collected from a UAV has a resolution in the order of centimetres and LiDAR can be collected at a point density of between 60-1,500 points m² (Puliti et al. 2015). However, due to range limitations UAVs are currently constrained for use to areas of up to 10 km² (Whitehead et al. 2014; Dandois and Ellis 2013), above which other data platforms (e.g. manned aircraft) become more cost effective at obtaining complete coverage (Heaphy et al. 2017). This restriction does limit the use of UAVs for major data acquisitions across large forest plantations. However, UAVs could play an important role in collection of data from small, scattered woodlots, or within plantation stands of a given age for a particular purpose (e.g. inventory, road planning) where an absence of high quality data can be economically and environmentally costly. Recent research also shows that partial sampling using UAVs in larger plantations could be a cost effective option for forest inventory (Puliti et al. 2018a).

The use of UAVs for forest inventory is one of the most promising applications of this technology. Three-dimensional point clouds are the most useful form of remotely sensed data for inventory purposes as these data have been reliably shown to accurately predict key forest biophysical variables such as height and volume in commercial forest settings (Dash et al. 2015; Watt and Watt 2013; Næsset 2002). Point clouds can be generated either through laser scanning (UAV-LS) (Jaakkola et al. 2010; Wallace et al. 2012) or through the use of imagery captured from digital still cameras (Dandois and Ellis 2013; Lisein et al. 2013). Laser scanning (LS) systems emit laser pulses and record the time-of-flight for reflected pulses. Combined with GNSS data on the sensors location, a three-dimensional point cloud representation of the scanned area can be produced. Three-dimensional representations can also be obtained using a combination of computer vision (Structure from Motion ; SfM) and photogrammetry techniques. These data will be referred to hereafter as SfM data. Unlike LiDAR, SfM methods rely on passive optical sensors that do not penetrate the canopy (Lowe 2004). Several authors have reported the predictive accuracy of models linking either UAV-SfM or UAV-LS data with ground reference forest biophysical properties (Dandois and Ellis 2013; Dandois et al. 2015; Wallace et al. 2016; Puliti et al. 2015; Lisein et al. 2013). Recent research also demonstrates the utility of explanatory variables derived from raw photogrammetric data and that do not require a digital terrain model (DTM) for prediction of forest volume (Giannetti et al. 2018). This is an approach that could be useful in situations where DTMs are not available. Despite this diverse range of UAV-based approaches to characterising forest inventory there is still a lack of understanding of how precision compares between these methods and to estimates obtained from only plot data.

The increasing availability of remotely sensed data has been matched by the development of sampling strategies to facilitate prediction of variables of interest in forest inventories. Traditional plot-based inventories use design-based inference, whereby a probability sample is taken from the

population according to an appropriate sampling design. The precision of the estimator is usually expressed through the variance, which is a fixed quantity given the population, sampling design and the estimator. The integration of point cloud data collected from UAVs with other sources of inventory information raises challenges for appropriate statistical inference and error estimation. The mode of inference used is governed by the area sampled which is primarily a function of the size of the resource, the UAV and sensor used for the survey and the available time and budget. For small forests, where complete coverage is possible, model-based variance estimators can be applied in the same manner as they are implemented for forest inventories that include a wall-to-wall coverage of remotely sensed auxiliary data from fixed wing aircraft or satellite (McRoberts et al. 2007). The precision of the estimators obtained from this form of inference are based on the uncertainty of the model parameter estimates (Gregoire 1998; McRoberts 2006, 2010). Further, cost-reductions can be obtained when auxiliary data is acquired only for a portion of the area of interest (AOI). In these cases the population parameters and the associated variance can be estimated through hybrid inference (Ståhl et al. 2016; Ståhl et al. 2010). Hybrid inference involves an initial collection of a probability sample of remotely sensed data and then a second sample of field plots. A great advantage of the hybrid inference for UAV applications is that the second sample (i.e., field plots) does not have to be a probability sample, thus field plots from outside the surveyed area can be included in the model development. The hybrid variance estimator includes both the sampling error in the first phase and the uncertainty due to parameter estimates (Ståhl et al. 2010).

The comparison of sampling strategies that include UAV data is clearly important for determining how this information can be most efficiently integrated into forest inventory. However, very little research has compared errors from design-based inference, using only plot data, to errors from model or hybrid inference that respectively integrate plot data with full and partial UAV coverage. Within a 7,330 ha forest area Puliti et al. (2017) compared the precision of hybrid estimation using partial-coverage UAV data and field plots to two other methods. These two methods included design-based inference using only field plots and a model-based approach that utilised wall-to-wall airborne laser scanning (ALS) data. Compared to the use of only field plots, the hybrid estimation using UAV data was 4.4 times more efficient. The largest precision was obtained through complete coverage of ALS data which had a relative efficiency 1.6 times greater than that obtained through use of the partial coverage UAV data. These results suggest that integration of partial UAV coverage with plot data may be a cost-effective and relatively precise inventory option for small woodlots (0-100 ha). However, we are unaware of any research that has undertaken a similar comparison of sampling strategies within small-moderate sized stands, with a high degree of stand uniformity, where complete coverage is possible from a UAV.

The research was undertaken in a small *Pinus radiata* D. Don (radiata pine) plantation located in the central North Island, New Zealand. Remotely sensed data used in analyses were extracted from the following four sources: (i) DTM-independent variables derived from photogrammetry (UAV-SfM), (ii) variables obtained from the normalized point cloud using a DTM from ALS and imagery (UAV-SfM_{DTM}) (iii), UAV point cloud data derived from laser scanning (UAV-LS) and (iv) ALS data (see Table 1 for summary). Explanatory variables obtained from these four sources were combined with plot data to generate stand level predictions of top height, stand density, basal area and total stem volume using model-based and hybrid inference. Precision for the four inventory variables was compared between design-based inference (using only plot data) and the eight possible combinations of data source (UAV-SfM, UAV-SfM_{DTM}, UAV-LS, ALS) and inferential frameworks (model-based, and hybrid inference) to identify the most efficient means of obtaining stand level estimates of the biophysical variables of interest.

Table 1: Description of datasets used to provide explanatory variables to model forest biophysical variables.

Dataset	Dataset Description
UAV-SfM	DTM-independent variables derived from UAV photogrammetry
UAV-SfM _{DTM}	Variables obtained from UAV imagery and the height-normalised SfM point cloud using a DTM acquired from ALS.
UAV-LS	Variables describing point cloud data derived from UAV laser scanning
ALS	Variables describing point cloud data derived from traditional airborne laser scanning

2. Materials

2.1. Study area

The study area, which was located close to Rotorua (38.235 S, 176.156 E, 380 masl) was a 40 ha radiata pine plantation established in 1993. The stand was pruned to 6 m and thinned from an initial density of ~600 stems per hectare (sph) to around 350 sph in a single thin-to-waste silvicultural intervention at age 9.

2.2. Field data

A total of 30 bounded circular 0.06 ha slope-adjusted field plots were measured to provide data for this study. The locations of these plots were selected according to a systematic grid with a spacing of 100 m × 100 m (Figure 1).



Figure 1. Overview of the sampling design for the acquisition of field data.

Plot measurements, which were taken during June 2017, included diameter at breast height (1.4 m), D , for all trees within the plot and height, H , on a sub-sample of eight suitable trees, covering the D range within the plot that were free from excessive lean or malformation. These measurements were used to fit a Petterson regression (Petterson 1955) using ordinary least square (OLS) between D and H for each plot that was subsequently used to estimate H for all plot trees where H was not measured. Top height was then calculated as the average height of the largest 100 trees per hectare, where largest was defined in terms of D . Plot basal area (G) and stand density (N) were calculated from the plot measurements. A compatible volume and taper equation (Goulding and Murray 1976) with coefficients derived from a nationwide dataset, was used to estimate stem volume and upper stem diameters based on the tree measurements recorded. These data were exposed to an optimal log-bucking algorithm embedded in a commercial forest yield prediction software package (YTGEN, Silmetra, Tokoroa, New Zealand). A set of log-grade specifications and prices provided by the forest manager were used to segregate trees into log-products using the log-bucking algorithm designed to maximize value. The total stem volume (TSV) was calculated for each plot by summing the total

volume assigned to both merchantable and non-merchantable log-products and dividing by the plot area (ha).

Summary statistics for all of the plots included in the study (Table 2) show relatively small variation in top height with mean of 36.3 m and range of 33.5 – 38.6 m. Mean values for N , G and TSV ranged almost two-fold across the plots (Table 2).

Table 2. Summary statistics for the ground reference data for top height (H), stand density (N), basal area (G), and total stem volume (TSV).

Variable	Mean	Range
Top Height (m)	36.3	33.5 – 38.6
Stand Density (stems ha ⁻¹)	366	233 – 450
Basal Area (m ² ha ⁻¹)	65.7	45.9 – 85.0
TSV (m ³ ha ⁻¹)	781	519 – 1007

2.3. Remotely sensed data

UAV Laser scanning data

Laser scanning data were acquired using a Velodyne HDL-32E (Velodyne, San Jose, USA) scanner embedded in a LidarUSA 'Snoopy A-Series' laser scanning system (LidarUSA, Alabama, USA). The laser scanner was mounted on an Altus ORC4 remotely piloted helicopter platform (Altus Ltd., Hamilton, New Zealand). A flying altitude of around 80 m above the local terrain was used and the flight plan ensured that there was significant side overlap to remove the possibility of data voids. All flight manoeuvres and altitude adjustments were made outside of the area of interest to avoid the possibility of flight artefacts in the dataset. The laser scanner is only capable of recording a single return but produced a pulse density of 712 pls/m² and a pulse spacing of 0.04 m.

Flight line matching, ground classification, noise removal, and the identification of overlap points were carried out in the Terrasolid software (Terrasolid Oy, Espoo, Finland). Subsequently, points classified as overlap were removed to ensure a more even density over the entire study area. A transect of the UAV-LS point cloud is provided in figure 2.

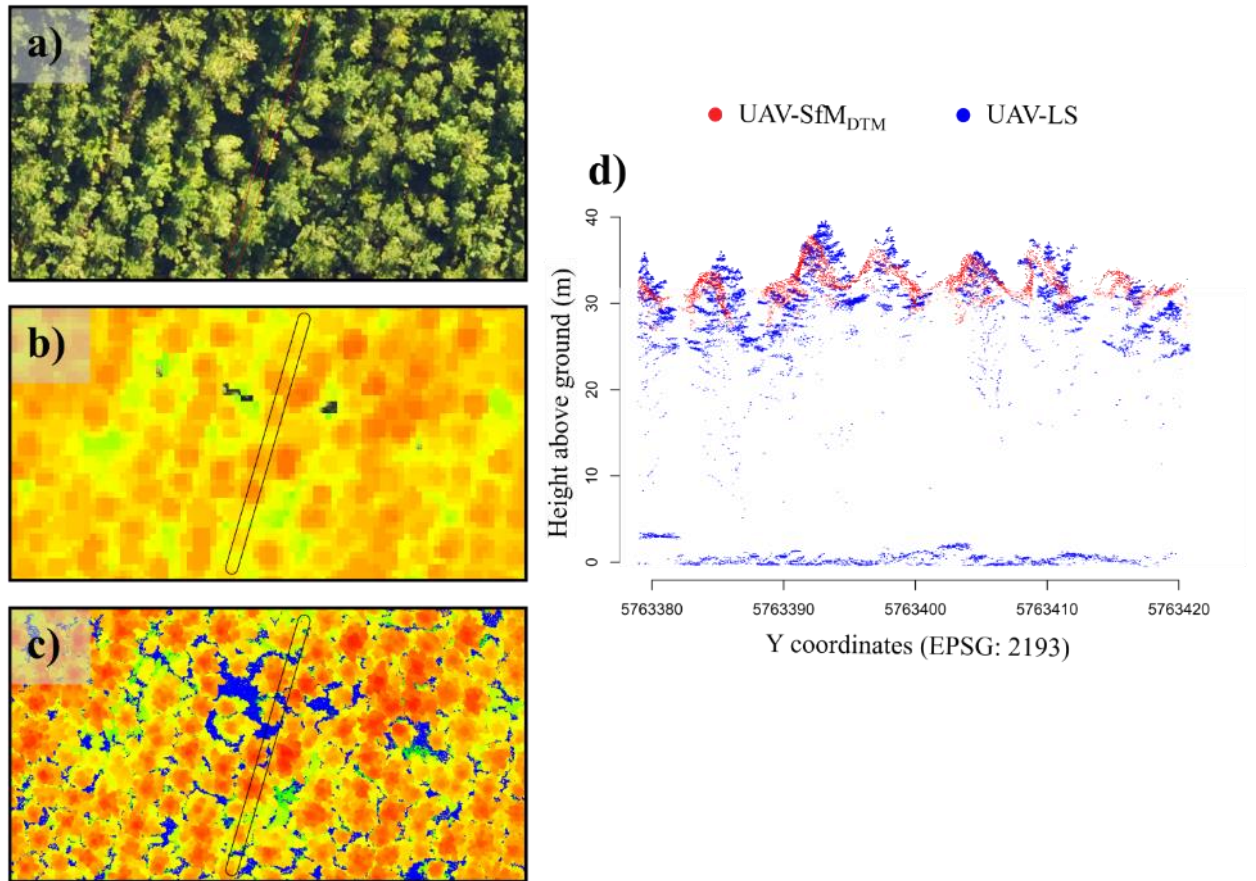


Figure 2. Detail of an area including a field plot to highlight the differences between the horizontal (a – c) and vertical (d) representations of the canopy using: a) the UAV orthomosaic (shown for visual reference only); b) the UAV-SfM canopy height model; c) the UAV-LS canopy height model; and d) the height normalised UAV-SfM and UAV-LS data.

A total of 28 ALS explanatory variables were calculated from the UAV-LS point cloud data coincident with the field plots. Extracted variables included height percentile ($p_{10}, p_{20}, \dots, p_{100}$), density variables ($d_{10}, d_{20}, \dots, d_{100}$), and the mean of 8 textural variables (mean, variance, homogeneity, contrast, dissimilarity, entropy, second moment, and correlation) calculated on the canopy height model using the R package 'gldm' (Zvloff 2016; Haralick et al. 1973). The UAV-LS data for the entire area was then tessellated using a grid of 600 m² cells for which the same variables as for the plots were then computed.

ALS data

The ALS data for this study was collected in December 2017 using a Trimble AX60i scanner with a Trimble AP50 inertial motion system and GNSS receiver. Campaign settings included a flying height of 700 m above ground level, pulse rate of 360 kHz and a swath side overlap of 60 %. The scanning system operated in multiple return mode and had an effective laser footprint size of 0.35 m. The resulting dataset had a pulse density of 10.2 pls/m² and an on ground point spacing of 0.31 m. Initial processing was carried out by the supplier in the Terrasolid software and included ground and noise classification using both automated and manual procedures. Subsequent processing was carried out in the LAsTools software package (RapidLasso GMBH, Gilching, Germany) and included triangulation of a terrain model using the ground classified points, further noise removal, and normalisation of elevations of non-ground returns to heights above the local ground level. The same variables that were extracted for the UAV-LS data were extracted for the ALS data.

UAV photogrammetric data

Full coverage imagery was acquired using a DJI ZenMuse X3 12MP camera (DJI, Shenzhen, China) mounted on a DJI Matrice 600 UAV. Dense overlapping images were acquired for the generation of point cloud data using Agisoft PhotoScan (Agisoft, 2017) adopting structure from motion. Flight altitude was set as 300 m above ground level and image overlap to 95 – 90 % front and side overlap. Imagery was collected under clear sky conditions within a single flight lasting 20 minutes. A total of five ground control points (GCPs) were established on the ground in open areas and/or canopy gaps and located using a Trimble Geo 7X differential GNSS system.

Photogrammetric processing of the UAV imagery resulted in a dense point cloud (approximately 60 points/m²) and an orthomosaic with a ground sampling distance of 10 cm. A total of 31 point cloud explanatory variables were extracted including height percentiles.

Two sets of variables were extracted from the UAV photogrammetric data, namely the UAV-SfM (i.e., DTM-independent) and the UAV-SfM_{DTM} variables (from the normalized point cloud). The former included a total of 163 explanatory variables extracted from the raw point cloud without any operations to alter the height values (i.e., normalization). These variables are further described in Giannetti et al. (2018). The latter variables included a total of 31 variables including height percentiles ($p_{10}, p_{20}, \dots, p_{100}$), density variables ($d_{10}, d_{20}, \dots, d_{100}$), the mean and standard deviation of textural variables calculated on the canopy height model using the R package 'glcm' (Zvoleff 2016) (*mean, variance, homogeneity, contrast, dissimilarity, entropy, second moment, correlation*) and the mean of the red, green and blue digital number values ($\bar{R}, \bar{G}, \bar{B}$).

3.Methods

3.1. Overview of sampling approach

The objective of this study was to estimate four forest biophysical variables (i.e., H , N , G and TSV) according to the following three different inventory cases that were relevant to small woodlots:

Case A: design-based inference using field plot data,

Case B: model-based inference using plot data and wall-to-wall coverage of UAV-SfM, UAV-LS or ALS data.

Case C: hybrid inference using plot data and partial coverage of UAV-SfM, UAV-LS, or ALS data.

Figure 3 illustrates these three different scenarios. Precision for the four biophysical variables was compared between the possible combinations of data source (UAV-SfM, UAV-SfM_{DTM}, UAV-LS, ALS) and estimators (Case A-design-based, Case B-model-based, and Case C-hybrid inference) to identify the most efficient means of obtaining estimates for the area of interest.

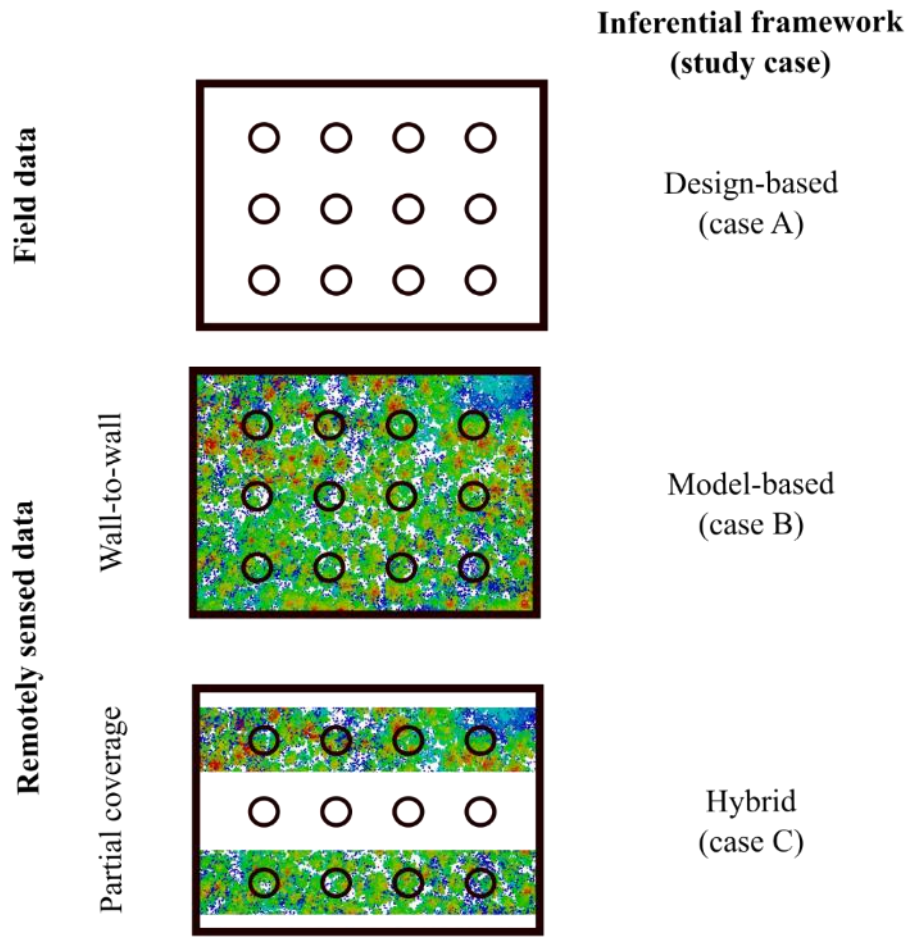


Figure 3. Visual representation of the different cases studied in terms of availability of field data and remotely sensed data coverage.

3.2. Development of models

For those cases where the inference relied on the use of remotely sensed auxiliary data (i.e., cases B and C) multiple linear regression models were developed. Separate models were developed for each of the variables of interest using the predictor variables extracted from either the UAV-LS, UAV-SfM, UAV-SfM_{DTM}, or ALS point cloud data. The variable selection was performed using a branch-and-bound search for the best subset of predictors using the leaps R-package (Lumley and Miller 2009). The search was restricted to models with a maximum of five variables. The model selection was performed using the Bayesian information criterion. The selection procedure was penalized for collinearity using the variance inflation factor. The subset with one variable less was iteratively selected if any of the variables in the current subset had a variance inflation factor ≥ 5 . The models were assessed by reporting the adjusted R^2 (R_{Adj}^2), the root mean square error ($RMSE$), the $RMSE$ as percentage of the mean ($RMSE_{\%}$), the mean difference (MD), and MD as percentage of the mean ($MD_{\%}$).

3.3. Inference

The following section describes in detail the estimators adopted in this study to estimate the mean for each of the studied forest biophysical properties ($\hat{\mu}$) and their variance ($\widehat{Var}(\hat{\mu})$) for a population U composed of N sampling units.

For case A assuming the field data (S) to represent a probability sample, a direct estimator of the mean is:

$$\hat{\mu}_A = \frac{1}{n} \sum_{i=1}^n y_{S_i} \quad (1)$$

where y_{S_i} is equal to the ground reference value of the biophysical variable of interest for the i th field plot ($i = 1, \dots, n$). The design-based variance of the mean ($\widehat{Var}(\hat{\mu}_A)$) was estimated using the variance estimator:

$$\widehat{Var}(\hat{\mu}_A) = \frac{\sigma_Y^2}{n(n-1)} \quad (2)$$

where σ_Y^2 is equal to the sample variance.

For cases B and C, multiple linear regression models linking the ground reference biophysical variable of interest with the explanatory variables extracted from the remotely sensed data (UAV-SfM or UAV-LS data) were fitted prior to the estimation. These had the form:

$$\mathbf{y}_S = \mathbf{K}_S \boldsymbol{\beta}_S \quad (3)$$

where \mathbf{K}_S is a $n \times r$ matrix, r is the number of selected explanatory variables, and $\boldsymbol{\beta}_S$ is the vector of model parameters of length $r + 1$. The OLS estimator of the model parameters is:

$$\hat{\boldsymbol{\beta}}_S = (\mathbf{K}_S^T \mathbf{K}_S)^{-1} \mathbf{K}_S^T \mathbf{y}_S \quad (4)$$

and the mean is estimated as:

$$\hat{\mu}_B = \boldsymbol{\iota}_U^T \mathbf{K}_U \hat{\boldsymbol{\beta}}_S \quad (5)$$

where $\boldsymbol{\iota}_U$ is a vector of length N where each element is equal to $1/N$ and \mathbf{K}_U is a $N \times (r + 1)$ matrix of explanatory variables from the remotely sensed auxiliary data. The variance estimator is:

$$\widehat{Var}(\hat{\mu}_B) = \boldsymbol{\iota}_U^T \mathbf{K}_U \mathbf{Cov}(\hat{\boldsymbol{\beta}}_S) \mathbf{K}_U^T \boldsymbol{\iota}_U \quad (6)$$

where $\mathbf{Cov}(\hat{\boldsymbol{\beta}}_S)$ is estimated according to:

$$\widehat{\mathbf{Cov}}(\hat{\boldsymbol{\beta}}_S) = \frac{\hat{\boldsymbol{g}}_S^T \hat{\boldsymbol{g}}_S}{n - r - 1} (\mathbf{K}_S^T \mathbf{K}_S)^{-1} \quad (7)$$

where $\hat{\boldsymbol{g}}_S$ is equal to a n -length vector of estimated residuals over the sample S .

For case C the estimation was performed according to a hybrid inferential framework using the sample S of ground reference data and a sample S_a of UAV strips composed of M grid cells. The same model developed in eq. 3 was applied to predict the biophysical variable of interest on the entire set of grid cells using:

$$\hat{\mathbf{y}}_{S_a} = \mathbf{Z}_{S_a} \hat{\boldsymbol{\beta}}_S \quad (8)$$

where \mathbf{Z}_{S_a} is equal to a $M \times (r + 1)$ matrix of UAV explanatory variables. The estimator of the population mean is:

$$\hat{\mu}_C = \boldsymbol{\iota}_{S_a}^T \mathbf{K}_{S_a} \hat{\boldsymbol{\beta}}_S \quad (9)$$

where $\boldsymbol{\iota}_{S_a}$ is a M -length vector of $1/M$ values. The variance estimator was estimated according to:

$$\widehat{Var}(\hat{\mu}_B) = \left(\frac{1}{M}\omega^2\right) + \mathbf{t}_{S_a}^T \mathbf{K}_{S_a} \mathbf{Cov}(\hat{\beta}_S) \mathbf{K}_{S_a}^T \mathbf{t}_{S_a} \quad (10)$$

where ω^2 is the sample-based variance for the vector of \hat{y}_{S_a} grid cells predictions, $\mathbf{Cov}(\hat{\beta}_S)$ is the covariance matrix of estimated models parameters derived using eq. 7.

3.4. Estimation of sampling statistics

The standard error (SE) was computed as the square root of the estimated variance and standard error as percentage of the mean ($SE_{\%}$). The relative efficiency (RE) was then computed as the ratio between the estimated variance under the design-based inference (i.e., case A) and that of each different case. The RE was then used to assess the number of field plots required to obtain the same level of precision as for each specific case. Thus, for the specific case where a total of $n = 30$ plots were used in case A, a value of $RE = 2$ would correspond to the need for twice the number of plots ($n = 60$) to obtain the same level of precision.

4. Results

4.1. Models

Tree height (H) was predicted with high accuracy by UAV-SfM_{DTM}, UAV-LS, and ALS with adjusted R^2 for these data sources ranging from 0.64 – 0.73 and $RMSE$ ranging from 0.76 – 0.91 m (Table 3). The upper percentiles (p_{90} , p_{95} , p_{100}) were the most important predictors within these models. In contrast, when UAV-SfM were used the quality of the model fit decreased ($R^2_{Adj} = 0.17$) and the $RMSE$ nearly doubled (1.33 m).

Stand density (N) was predicted with largest accuracy by UAV-SfM_{DTM} ($R^2_{Adj} = 0.69$), moderate accuracy by UAV-LS ($R^2_{Adj} = 0.57$) and UAV-SfM ($R^2_{Adj} = 0.55$) but only weak accuracy by ALS ($R^2_{Adj} = 0.34$). Important variables used within these models included height percentiles and density variables from the mid to upper height range as well as textural variables describing horizontal height variations in the point cloud (see Table 3).

For basal area (G) use of UAV photogrammetric data (UAV-SfM or UAV-SfM_{DTM}) produced a better model fit (R^2_{Adj} ranging from 0.49 to 0.63) than UAV-LS or ALS data (R^2_{Adj} ranging from 0.21 to 0.33). For the three datasets acquired from the UAV, density and textural variables were most useful for predicting G while the ALS derived model used only d_{100} .

As with basal area, total stem volume (TSV) was most accurately predicted using UAV-SfM_{DTM} ($R^2_{Adj} = 0.65$) and UAV-SfM ($R^2_{Adj} = 0.57$) while the fit quality decreased when UAV-LS ($R^2_{Adj} = 0.45$) or ALS ($R^2_{Adj} = 0.37$) were used instead. A mixture of density, percentile and textural variables were selected as predictors of TSV for the three UAV acquired datasets (Table 3).

Overall, it was noteworthy that textural variables were selected in nearly 60% of the models.

Table 3. Summary of the developed models using all the field observation

Variable of interest	Auxiliary data	Explanatory variables ^a	R^2_{Adj}	$RMSE^*$	$RMSE_{\%}^*$	MD^*	$MD_{\%}^*$
<i>H</i>	UAV-SfM	$n_{intensity_{1Q}}$	0.17	1.33	3.68	0.00	-0.01
	UAV-SfM _{DTM}	p_{95}, \overline{crown}	0.73	0.76	2.08	0.01	0.02
	UAV-LS	p_{95}, p_{100}	0.72	0.76	2.11	0.001	0.006
	ALS	$p_{90}, \overline{ntrees}$	0.64	0.91	2.50	-0.02	-0.05
<i>N</i>	UAV-SfM	$SD_{dissimilarity}, \overline{max_{green}}$	0.55	38.22	10.44	0.70	0.19
	UAV-SfM _{DTM}	$d_{90}, \overline{blue}, \overline{SD_{dissimilarity}}$	0.69	34.06	9.34	0.16	0.04
	UAV-LS	$p_{30}, \overline{d_{50}}, \overline{homogeneity}, \overline{second\ moment}$	0.57	39.8	10.87	-0.11	-0.03
	ALS	p_{60}	0.34	45.96	12.55	-0.36	-0.09
<i>G</i>	UAV-SfM	$\overline{mean}, \overline{homogeneity}$	0.49	5.54	8.42	-0.05	-0.07
	UAV-SfM _{DTM}	$d_{90}, d_{100}, \overline{dissimilarity}, \overline{SD_{mean}}, \overline{SD_{variance}}$	0.63	4.97	7.55	0.15	0.23
	UAV-LS	$\overline{variance}$	0.21	7.01	10.66	-0.008	-0.008
	ALS	d_{100}	0.33	6.36	9.67	-0.05	-0.08
<i>TSV</i>	UAV-SfM	$\overline{mean}, \overline{homogeneity}$	0.57	62.75	8.04	-0.54	-0.07
	UAV-SfM _{DTM}	$p_{95}, d_{100}, \overline{mean}, \overline{dissimilarity}$	0.65	60.57	7.76	-0.55	-0.07
	UAV-LS	$d_{10}, d_{90}, \overline{mean}$	0.45	77.58	9.93	-2.02	-0.25
	ALS	p_{30}	0.37	75.99	9.73	-0.55	-0.07

a .

 $n_{intensity_{1Q}}$: number of points within the first quartile of intensity value (see Giannetti et al. 2018) \overline{ntrees} : average number of local maxima \overline{crown} : average crown size $\overline{max_{green}}$: maximum green value \overline{blue} : mean blue value $p_{10}-p_{100}$: height percentiles $d_{10}-d_{100}$: density variables $\overline{mean}, \overline{homogeneity}, \overline{second\ moment}, \overline{dissimilarity}, \overline{variance}$: mean textural variables $SD_{dissimilarity}$: standard deviation textural variables

4.2. Relative efficiency

Results from the estimation showed that use of remotely sensed data nearly always increased the precision of design-based estimates using only field plot data (Table 4; Figure 5a). For case B the average *RE* for all remotely sensed data sources for *H*, *N*, *G*, and *TSV* were 1.77, 1.47, 1.10 and 1.27, respectively. Gains in *RE* for *N*, *G*, and *TSV* were largest using data from UAV-SfM_{DTM} and *RE* values were respectively, 1.96, 1.39 and 1.65 (Table 4; Figure 5a). In contrast, gains in *RE* for *H* were largest using UAV-LS (*RE* = 3.02) and ALS (*RE* = 2.06) but very low or non-existent using photogrammetric point cloud data (*RE* range = 0.95 – 1.05). Gains using ALS were consistent across *N*, *G*, and *TSV* and were larger than those achieved using UAV-LS for *N* (*RE* = 1.28 vs 1.13), *G* (*RE* = 1.2 vs 0.86), and *TSV* (*RE* = 1.28 vs 1.04). Values of *RE* for UAV-SfM were markedly higher than those of UAV-LS for *N* (*RE* = 1.49 vs 1.13) but only marginally larger for *G* (*RE* = 0.93 vs 0.86) and *TSV* (*RE* = 1.12 vs 1.04).

Table 4. Result of the estimation of the studied biophysical variables of interest according to the studied cases (A, B, C) and data sources in terms of estimated mean ($\hat{\mu}$), variance of the mean ($\widehat{Var}(\hat{\mu})$), standard error (SE), standard error as a percentage of the estimated mean for case A ($SE_{\%}$), relative efficiency as a ratio between $\widehat{Var}(\hat{\mu})$ for case A and the $\widehat{Var}(\hat{\mu})$ for the respective case.

Variable of interest	Data used in the estimation	Cases	$\hat{\mu}$	$\widehat{Var}(\hat{\mu})$	SE	$SE_{\%}$	RE	n^*	
H	Field plots	A	36.3	0.07	0.3	0.7	1.00	30	
		B	36.1	0.07	0.3	0.7	0.95	29	
	UAV-SfM	C	36.2	0.08	0.3	0.8	0.88	27	
		B	36.9	0.06	0.3	0.7	1.05	31	
	UAV-SfM _{DTM}	C	36.8	0.08	0.3	0.8	0.80	24	
		B	36.2	0.02	0.2	0.4	3.02	91	
	UAV-LS	C	36.3	0.04	0.2	0.5	1.79	54	
		B	36.4	0.03	0.2	0.5	2.06	62	
	ALS	C	36.4	0.04	0.2	0.5	1.70	51	
		A	366.1	98.65	9.9	2.7	1.00	30	
	N	Field plots	B	355.9	66.14	8.1	2.2	1.49	45
			C	353.1	88.94	9.4	2.6	1.11	33
UAV-SfM		B	362.0	50.23	7.1	1.9	1.96	59	
		C	360.4	75.91	8.7	2.4	1.30	39	
UAV-SfM _{DTM}		B	346.2	87.08	9.3	2.7	1.13	34	
		C	349.1	118.67	10.9	3.0	0.83	25	
UAV-LS		B	361.0	77.36	8.8	2.4	1.28	38	
		C	363.2	86.41	9.3	2.5	1.14	34	
G		Field plots	A	65.8	1.84	1.4	2.1	1.00	30
			B	62.6	1.97	1.4	2.1	0.93	28
		UAV-SfM	C	63.2	2.13	1.5	2.2	0.86	26
			B	64.4	1.32	1.1	1.7	1.39	42
	UAV-SfM _{DTM}	C	65.2	1.69	1.3	2.0	1.09	33	
		B	64.1	2.14	1.5	2.2	0.86	26	
	UAV-LS	C	65.5	8.34	2.9	4.4	0.22	7	
		B	64.7	1.53	1.2	1.9	1.20	36	
	ALS	C	65.3	1.62	1.3	1.9	1.14	34	
		A	780.9	282.63	16.8	2.2	1.00	30	
	TSV	Field plots	B	739.1	253.34	15.9	2.0	1.12	33
			C	746.0	292.43	17.1	2.2	0.97	29
UAV-SfM		B	769.0	170.96	13.1	1.7	1.65	50	
		C	775.9	225.63	15.0	1.9	1.25	38	
UAV-SfM _{DTM}		B	782.8	271.11	16.5	2.1	1.04	31	
		C	784.3	320.0	17.9	2.3	0.88	26	
UAV-LS		B	765.9	220.85	14.9	1.9	1.28	38	
		C	772.5	241.48	15.5	2.0	1.17	35	

* n = number of plots required to obtain the same level of precision as using field data alone

Relative efficiency was larger when auxiliary data were available on a wall-to-wall basis as in case B rather than partial-coverage in case C (Table 4, Figure 4b). Despite the poorer performance of case C, the variation in RE followed a similar trend to that of case B. Gains in RE were greatest for H using either ALS or UAV-LS ($RE = 1.7 - 1.79$) but RE from these sources were markedly reduced from values obtained in case B (Fig. 4a). Values of RE were largest using either UAV-

SfM_{DTM} or ALS for N ($RE = 1.30$ and 1.14), G ($RE = 1.09$ and 1.14) and TSV ($RE = 1.25$ and 1.17) but values of RE for UAV-SfM and UAV-LS were most often below one for these three variables (Fig. 4b).

The use of predictor variables extracted from a normalized photogrammetric point cloud (i.e., UAV-SfM_{DTM}) resulted in larger RE than use of DTM-independent variables (i.e., UAV-SfM) for almost all biophysical variables and sampling methods. Using wall-to-wall UAV-SfM_{DTM} data provided marked gains over UAV-SfM for N (1.96 vs 1.49), G (1.39 vs 0.93) and TSV (1.65 vs 1.12) (Fig. 4a) but these differences were reduced when using partial-coverage data to estimate these variables (Fig. 4b). Gains were least marked for H in cases B and C and RE values for both these cases were close to or less than 1 (Fig. 4a, b).

Differences in RE between ALS or UAV-LS varied between biophysical variables. For case B the use of UAV-LS was more efficient than ALS ($RE = 3.02$ vs 2.06) but this difference diminished greatly for case C ($RE = 1.79$ vs 1.70). In contrast, for both cases B and C, the use of ALS resulted in larger RE than for UAV-LS when estimating N , G and TSV . These differences were most marked for case C (Fig. 4a, b). The RE obtained from ALS always exceeded one but values of RE obtained from UAV-LS were smaller than one for 50% of all eight tested combinations of data sources and sampling methods (Fig. 4a,b).

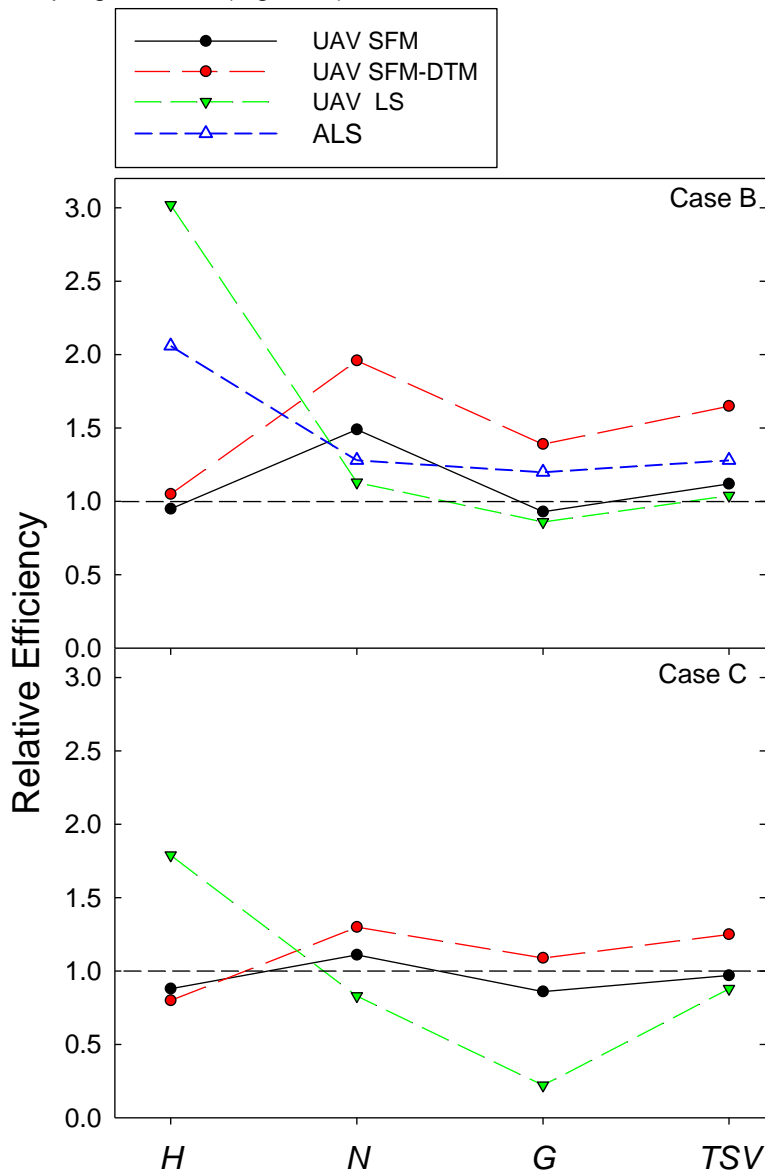


Figure 4. Variation in relative efficiency for all four variables of interest (H , N , G and TSV), between the four data sources (see legend), for (top) case B - wall-to-wall auxiliary and (bottom) case C - hybrid inference.

5. Discussion

The use of remotely sensed UAV auxiliary data in the estimation, either from laser scanning or photogrammetric data, were found to provide gains over a purely field-based estimate. Despite this, gains reported here using model-based inference were relatively low compared to previous research that has shown RE of 7.4 (Puliti et al. 2017) for volume using ALS data as the auxiliary variable. These modest gains in RE are likely to reflect the relatively homogenous nature of the sampled stand and the relatively higher sampling intensity of field data compared to previous studies. The lower variation in stand biophysical variables, associated with a rather high sampling intensity, resulted in poorer precision of the design-based estimate and reduced model performance. As a result, the RE for cases B and C was relatively conservative and at the lower end of the expected range for estimates that include remotely sensed data.

Unsurprisingly, case B was considerably more efficient than case C. This was expected as the complete cover of auxiliary data that was available in case B eliminated the first-phase sampling error which was present in case C. Case C was on average only marginally (mean $RE = 1.06$) more efficient than use of field based plots. Few studies have compared these two methods in the literature. Puliti *et al.* (2017) found hybrid inference produced only modest gains in RE over field based estimation ($RE = 1.2$) within a much larger forest. However these gains significantly increased when plots external to the study area were included ($RE = 4.4$) highlighting the potential for model enhancement through inclusion of additional inventory data (Puliti et al. 2017).

Our results and previous findings (Puliti et al. 2017) suggest hybrid inference, using auxiliary data from a UAV, is likely to be most cost-effective for characterising forests of moderate size with many field plots for two reasons. Under these circumstances, partial data collection using a UAV may represent a cost-effective means of acquiring auxiliary data, particularly if the stand is too large to be completely flown by UAV but too small to justify an ALS acquisition. Secondly, as model error for the hybrid estimator diminishes with increasing plot number (Puliti et al. 2017), the higher number of plots associated with forests of moderate size is likely to favour hybrid inference.

Recent research has demonstrated the utility of DTM-independent variables derived from photogrammetry for prediction of volume (Giannetti et al. 2018). Using data from two forests in Italy and Norway, volume was predicted with very similar respective precision using ALS variables ($R^2 = 0.79$ and 0.79), UAV-SfM_{DTM} (0.83 and 0.80), and UAV-SfM (0.70 and 0.79) (Giannetti et al. 2018). Our results extend this approach to a broader range of inventory variables and investigate the utility of UAV-SfM for improving RE . Compared to UAV-SfM_{DTM} we found models using UAV-SfM to have reduced predictive accuracy, particularly for H , but also to a lesser extent for all other variables including TSV . This reduced predictive accuracy translated into smaller RE values from UAV-SfM compared to UAV-SfM_{DTM}. Despite the larger uncertainty compared to UAV-SfM_{DTM}, UAV-SfM variables generally yielded similarly precise estimates to those using more advanced laser scanning data. Given that UAV-SfM inventories are easier to implement, as they do not require a DTM, research should further explore the use of this approach at prediction of biophysical variables across a range of forest types and stand conditions.

Although models had a similar precision, the use of LiDAR collected from a UAV provided significantly more precise estimates of RE for tree height than use of UAV-SfM_{DTM}. This broadly agrees with findings by Wallace et al., (2016) who showed UAV-LS to be more accurate ($RMSE = 0.92$ m) than UAV-SfM_{DTM} ($RMSE = 1.30$ m) for prediction of height. Results from this study extended the comparison between these two UAV data sources to N , G , and TSV which, in contrast to H , showed higher RE for models developed from UAV-SfM_{DTM} than those developed from UAV-LS data. It is important to note that the UAV laser scanning sensor used in this study was a consumer-grade sensor developed primarily for the automotive industry. As a result, some of the intrinsic characteristics of these sensors limits their application for forest inventory purposes. As with most consumer-grade laser scanners, the beam divergence is rather large which strongly restricts the ability of the laser beam to penetrate through small canopy gaps. Further research should examine how predictions made using UAV-SfM_{DTM} compare to those from survey-grade laser scanners (e.g., Riegl VUX-1UAV), which can penetrate more deeply into the canopy and have a higher number of returns per outgoing pulse.

In conclusion, our results support the use of model-based estimation in small woodlots that are homogenous in structure. As well as being more precise than hybrid inference, model-based estimation has the advantage that it does not require a probability sample from the target area (Ståhl et al. 2016) and that variance estimators are not overly sensitive to geolocation mismatches between field plots and the auxiliary data (Saarela et al. 2016). The results indicate that the collection of partial-coverage auxiliary data should be considered an option only for rather large areas where reducing the auxiliary area coverage translates into a significant reduction in the time required for UAV operations. UAV-SfM_{DTM} data yielded some of the most precise estimates out of the studied data sources and variables of interest, highlighting the relevance of using UAV photogrammetric data for estimation of key variables such as N , G , and TSV .

References

- Agisoft (2017). Agisoft PhotoScan User Manual: Professional Edition, Version 1.3.
- Dandois, J. P., & Ellis, E. C. (2013). High spatial resolution three-dimensional mapping of vegetation spectral dynamics using computer vision. *Remote Sensing of Environment*, 136, 259-276.
- Dandois, J. P., Olano, M., & Ellis, E. C. (2015). Optimal altitude, overlap, and weather conditions for computer vision UAV estimates of forest structure. *Remote Sensing*, 7(10), 13895-13920.
- Dash, J. P., Marshall, H. M., & Rawley, B. (2015). Methods for estimating multivariate stand yields and errors using k-NN and aerial laser scanning. *Forestry*.
- Dash, J. P., Watt, M. S., Pearse, G. D., Heaphy, M., & Dungey, H. S. (2017). Assessing very high resolution UAV imagery for monitoring forest health during a simulated disease outbreak. *ISPRS journal of photogrammetry and remote sensing*, 131, 1-14.
- Giannetti, F., Chirici, G., Gobakken, T., Næsset, E., Travaglini, D., & Puliti, S. (2018). A new approach with DTM-independent metrics for forest growing stock prediction using UAV photogrammetric data. *Remote Sensing of Environment*, 213, 195-205.
- Goodbody, T. R. H., Coops, N. C., Tompalski, P., Crawford, P., & Day, K. J. K. (2017). Updating residual stem volume estimates using ALS- and UAV-acquired stereo-photogrammetric point clouds. *International Journal of Remote Sensing*, 38(8-10), 2938-2953, doi:10.1080/01431161.2016.1219425.
- Goulding, C., & Murray, J. (1976). Polynomial taper equations that are compatible with tree volume equations. *NZJ For. Sci*, 5(3), 313-322.
- Gregoire, T. G. (1998). Design-based and model-based inference in survey sampling: appreciating the difference. *Canadian journal of forest research*, 28(10), 1429-1447.
- Haralick, R. M., Shanmugam, K., & Dinstein, I. H. (1973). Textural features for image classification. *Systems, Man and Cybernetics, IEEE Transactions on*(6), 610-621.
- Heaphy, M., Watt, M. S., Dash, J. P., & Pearse, G. D. (2017). UAVs for data collection - plugging the gap. *New Zealand Journal of Forestry Science*, 62 (1).
- Hughenoltz, C. H., Moorman, B. J., Riddell, K., & Whitehead, K. (2012). Small unmanned aircraft systems for remote sensing and earth science research. *Eos, Transactions American Geophysical Union*, 93(25), 236-236.
- Jaakkola, A., Hyyppä, J., Kukko, A., Yu, X., Kaartinen, H., Lehtomäki, M., & Lin, Y. (2010). A low-cost multi-sensoral mobile mapping system and its feasibility for tree measurements. *ISPRS Journal of Photogrammetry and Remote Sensing*, 65(6), 514-522, doi:https://doi.org/10.1016/j.isprsjprs.2010.08.002.
- Lisein, J., Pierrot-Deseilligny, M., Bonnet, S., & Lejeune, P. (2013). A Photogrammetric Workflow for the Creation of a Forest Canopy Height Model from Small Unmanned Aerial System Imagery. *Forests*, 4(4), 922.
- Lowe, D. G. (2004). Method and apparatus for identifying scale invariant features in an image and use of same for locating an object in an image. Google Patents.
- Lumley, T., & Miller, A. (2009). Leaps: Regression Subset Selection. Available at: <http://cran.r-project.org/web/packages/leaps/leaps.pdf>.
- McRoberts, R. E. (2006). A model-based approach to estimating forest area. *Remote Sensing of Environment*, 103(1), 56-66.
- McRoberts, R. E. (2010). Probability-and model-based approaches to inference for proportion forest using satellite imagery as ancillary data. *Remote Sensing of Environment*, 114(5), 1017-1025.

- McRoberts, R. E., Tomppo, E. O., Finley, A. O., & Heikkinen, J. (2007). Estimating areal means and variances of forest attributes using the k-Nearest Neighbors technique and satellite imagery. *Remote Sensing of Environment*, 111(4), 466-480.
- Næsset, E. (2002). Predicting forest stand characteristics with airborne scanning laser using a practical two-stage procedure and field data. *Remote Sensing of Environment*, 80(1), 88-99, doi:https://doi.org/10.1016/S0034-4257(01)00290-5.
- Nex, F., & Remondino, F. (2014). UAV for 3D mapping applications: a review. *Applied Geomatics*, 6(1), 1-15.
- Petterson, H. (1955). Yield of coniferous forests. *Medd. Stat. Skogsforsöksanst.*, 45.
- Pierzchała, M., Talbot, B., & Astrup, R. (2014). Estimating Soil Displacement from Timber Extraction Trails in Steep Terrain: Application of an Unmanned Aircraft for 3D Modelling. *Forests*, 5(6), 1212.
- Puliti, S., Ene, L. T., Gobakken, T., & Næsset, E. (2017). Use of partial-coverage UAV data in sampling for large scale forest inventories. *Remote Sensing of Environment*, 194, 115-126.
- Puliti, S., Ørka, H. O., Gobakken, T., & Næsset, E. (2015). Inventory of small forest areas using an unmanned aerial system. *Remote Sensing*, 7(8), 9632-9654.
- Puliti, S., Saarela, S., Gobakken, T., Ståhl, G., & Næsset, E. (2018a). Combining UAV and Sentinel-2 auxiliary data for forest growing stock volume estimation through hierarchical model-based inference. *Remote Sensing of Environment*, 204(Supplement C), 485-497, doi:https://doi.org/10.1016/j.rse.2017.10.007.
- Puliti, S., Talbot, B., & Astrup, R. (2018b). Tree-Stump Detection, Segmentation, Classification, and Measurement Using Unmanned Aerial Vehicle (UAV) Imagery. *Forests*, 9(3), 102.
- Saarela, S., Schnell, S., Tuominen, S., Balázs, A., Hyyppä, J., Grafström, A., & Ståhl, G. (2016). Effects of positional errors in model-assisted and model-based estimation of growing stock volume. *Remote Sensing of Environment*, 172, 101-108.
- Salamí, E., Barrado, C., & Pastor, E. (2014). UAV flight experiments applied to the remote sensing of vegetated areas. *Remote Sensing*, 6(11), 11051-11081.
- Ståhl, G., Holm, S., Gregoire, T. G., Gobakken, T., Næsset, E., & Nelson, R. (2010). Model-based inference for biomass estimation in a LiDAR sample survey in Hedmark County, Norway This article is one of a selection of papers from Extending Forest Inventory and Monitoring over Space and Time. *Canadian journal of forest research*, 41(1), 96-107.
- Ståhl, G., Saarela, S., Schnell, S., Holm, S., Breidenbach, J., Healey, S. P., Patterson, P. L., Magnussen, S., Næsset, E., McRoberts, R. E., & Gregoire, T. G. (2016). Use of models in large-area forest surveys: comparing model-assisted, model-based and hybrid estimation. [journal article]. *Forest Ecosystems*, 3(1), 5, doi:10.1186/s40663-016-0064-9.
- Talbot, B., Rahlf, J., & Astrup, R. (2017). An operational UAV-based approach for stand-level assessment of soil disturbance after forest harvesting. *Scandinavian Journal of Forest Research*, 1-10, doi:10.1080/02827581.2017.1418421.
- Wallace, L., Lucieer, A., Malenovsky, Z., Turner, D., & Vopěnka, P. (2016). Assessment of Forest Structure Using Two UAV Techniques: A Comparison of Airborne Laser Scanning and Structure from Motion (SfM) Point Clouds. *Forests*, 7(3), 62.
- Wallace, L., Lucieer, A., Watson, C., & Turner, D. (2012). Development of a UAV-LiDAR System with Application to Forest Inventory. *Remote Sensing*, 4(6), 1519.
- Watt, M. S., Heaphy, M., Dunningham, A., & Rolando, C. (2017). Use of remotely sensed data to characterise weed competition in forest plantations. *International Journal of Remote Sensing* 38, 2448-2463.
- Watt, P. J., & Watt, M. S. (2013). Development of a national model of tree volume from LiDAR metrics for New Zealand. *Remote Sensing of Environment*, 34, 5892-5904.
- Watts, A. C., Ambrosia, V. G., & Hinkley, E. A. (2012). Unmanned aircraft systems in remote sensing and scientific research: Classification and considerations of use. *Remote Sensing*, 4(6), 1671-1692.
- Whitehead, K., & Hugenholtz, C. H. (2014). Remote sensing of the environment with small unmanned aircraft systems (UASs), part 1: A review of progress and challenges 1. *Journal of Unmanned Vehicle Systems*, 2(3), 69-85.
- Whitehead, K., Hugenholtz, C. H., Myshak, S., Brown, O., LeClair, A., Tamminga, A., Barchyn, T. E., Moorman, B., & Eaton, B. (2014). Remote sensing of the environment with small unmanned aircraft systems (UASs), part 2: scientific and commercial applications 1. *Journal of Unmanned Vehicle Systems*, 2(3), 86-102.
- Zvoleff, A. (2016). Package 'glcm'. (1.6.1 ed.).

Theme 2: A Community Approach – Plot sharing to provide the benefits of large scale to Woodlot growers

Background

Remote sensing has been applied to forest management since the 1950s when imagery collected from aircraft was first applied to update estimates of forest area. Since the advent of the development of airborne laser scanning (ALS, also commonly referred to as Lidar) these data have formed a significant part of national and stand-level forest inventories in many countries. The widespread adoption of these methods around the world are evidence of their efficacy. In New Zealand partial coverage ALS surveys constitute a part of a national carbon inventory maintained by the Ministry of the Environment (LUCAS) and are now collected fairly routinely by the managers of larger commercial forests. Research into using ALS data for forest inventory has delivered the technology as a practical tool for the managers of large estates but growers of smaller forests are typically excluded from accessing some of these benefits. This is due to several factors including the statistical modelling technique employed, and the cost of acquiring remotely sensed data.

A statistical modelling approach called k nearest neighbour (k-NN) imputation was shown to be highly suitable for application to New Zealand forestry (Dash et al, 2015) and has since been applied to many large forests in New Zealand and Australia with considerable success. Key advantages of the approach include multivariate yield prediction, the ability to provide yield estimates that are additive and consistent, and independence from a specific software package or yield modelling pathway. These features make the approach particularly suitable for the information requirements of forest inventory and yield table development. Despite these favourable attributes a negative aspect of the approach is the requirement for a relatively large sample size. When using this non-parametric method it is particularly important that the full range of growing conditions in a forest resource are sampled in the reference dataset used for model development and neighbour selection. This is more important than for more conventional parametric methods because k-NN cannot be used to extrapolate beyond the range of the training dataset. As forest variability is not linearly related to forest area the required sampling intensity for smaller forests may be much higher than for larger forests. This leads to inefficiencies when applying this approach to smaller forests and below a certain size threshold this would make the adoption of this approach cost-prohibitive.

The cost of acquiring ALS data has decreased significantly in recent years to the extent where it is now a very appealing data source for terrain modelling and forest inventory. However the cost of ALS acquisition is a function of the size, shape, and location of the target forest with the cost per hectare significantly influenced by forest area. This is largely due to the costs of initialising a survey and competition amongst suppliers to secure large scale data collection contracts. As a result ALS data is usually significantly more expensive for small-forest growers seeking to commission their own survey. In order to access ALS survey data small-forest growers can potentially collaborate to share costs and reduce the price of data collection on a per-hectare basis. However, this requires significant organisation and foresight. Alternatively small-forest growers can make use of the growing inventory of open access datasets. These data are typically collected by central, or regional, government usually for non-forestry purposes. The capture properties of these data vary considerably but a significant proportion are suitable for use in forest inventory or forest terrain modelling. Despite significant support New Zealand does not currently have wall-to-wall national coverage of open access data but the area covered is sizeable and increasing (Figure 1). A database of the available open access ALS data was queried to produce Figure 1 and guide selection of a case study region.

Significant areas in the Bay of Plenty and Southern North Island (SNI) are covered by open access data and represented good options for the case study location as these regions contain a large number of small-plantations. After examination of the data the SNI was selected as a suitable case study location as the open access data available here is relatively current and is of a reasonable density and quality.

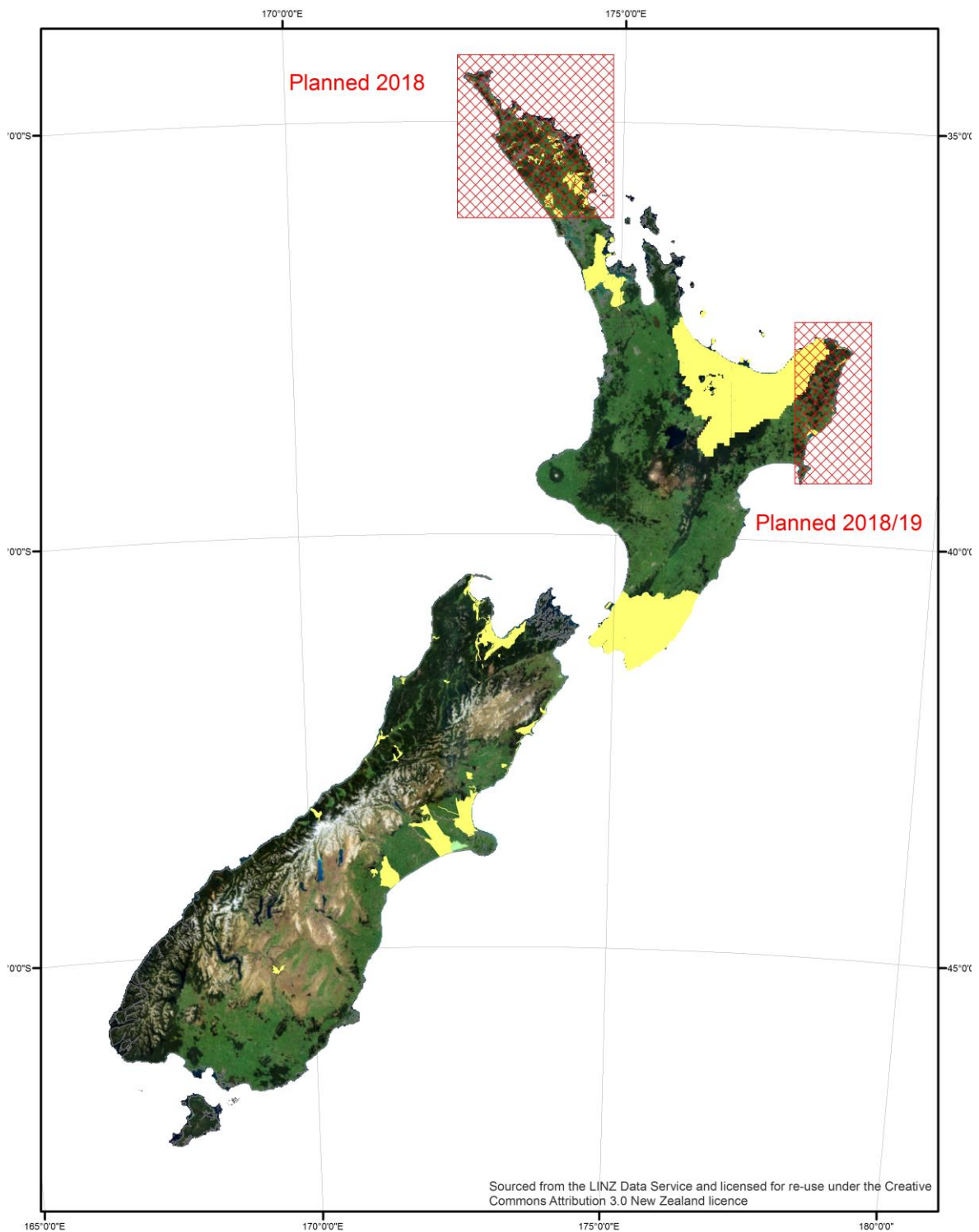
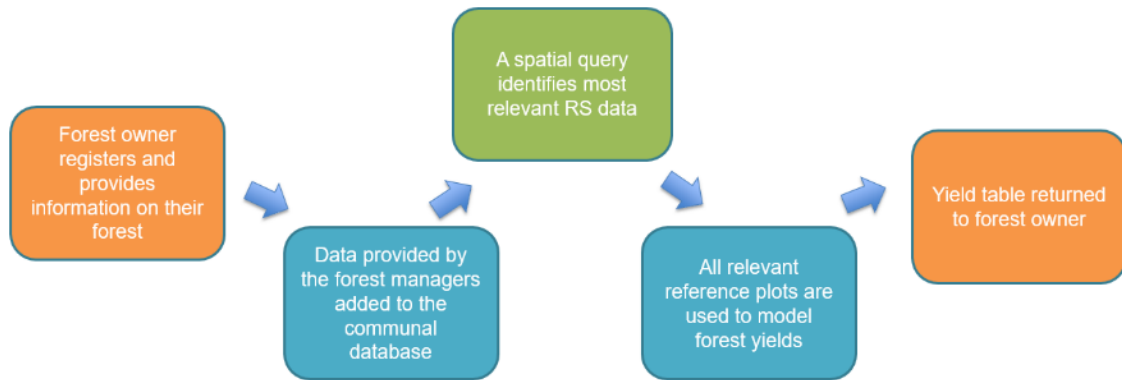


Figure 1. The location of the current open access ALS data available in New Zealand (shown in yellow) with the location of two major planned regional government acquisitions shown in red hatching. The base maps shows a cloud free mosaic from ESA Sentinel 2.1A satellite.

Within the SNI we installed a case study to examine the feasibility of a community plot sharing approach for small-forest growers and developed a prototype analysis framework for how a system such as this might work in practice. The framework we developed and implemented is summarised in the figure below.



Objectives

The objectives of case study were:

1. To examine open access ALS data sources and methods for large-scale processing.
2. To raise awareness that a data sharing approach is a feasible possibility for small-forest growers.
3. To install a case study describing how a community data sharing framework might operate.
4. Investigate what the outputs of such a framework might be and how these might be made available to small-forest growers.

Case study

The methods that we followed and results obtained from the case study are outlined in the following sections.

Study site

Following assessment of the available datasets the Southern North Island was selected as the study area of interest (Figure 2). This area was chosen due to the availability of a remote sensing dataset and the presence of a significant quantity of small to medium sized plantation forests in the area. The study area (804,800 ha) included all districts in the greater Wellington area including Wairarapa, Carterton, Masterton, Wellington, Upper Hutt, and Kapiti coast. The climate of this region is temperate and relatively dry, with annual rainfall ranging from 800 to 1,200 millimetres and maximum temperatures of 20–28 °C in summer and 10–15 °C in winter. According to the National Exotic Forest Description the plantation forests in the area are primarily radiata pine (98 %) with the balance planted in Douglas fir, and cypress species.

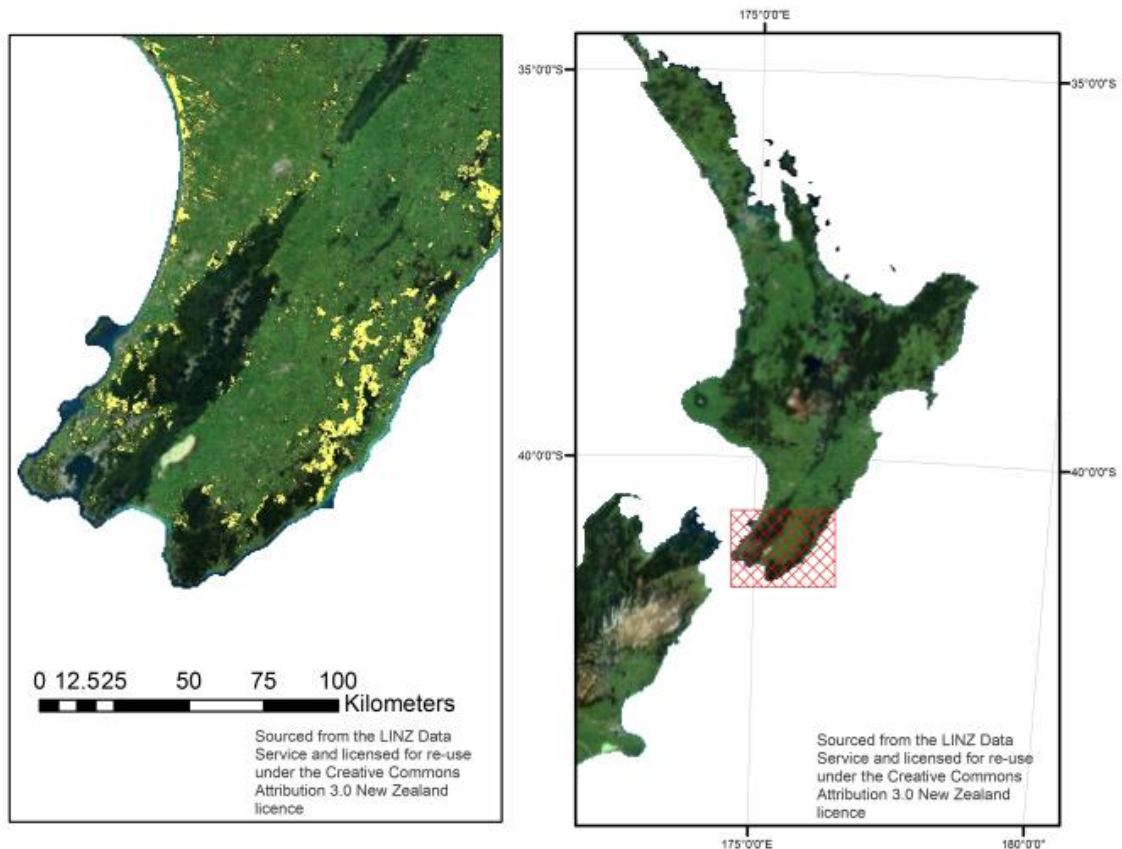


Figure 2. The right hand panel shows the study area (red hatching). The left hand panel shows a zoomed in view of the study area with areas covered in planted forest (Source = LCDB) shown in yellow.

Plot data acquisition

A central objective of this research was to engage growers of small forests, make them aware that this type of approach is possible, and encourage them to share their data where appropriate. Farm foresters in New Zealand are a large and diverse group and contacting them turned out to be a challenging process. We publicised the project and invited participants to provide data through publications in the NZ Farm Forestry Associations “Tree Grower”, Friday Offcuts weekly newsletter, Scion’s Connections newsletter, and through presentations at a Forest Growers Research conference and via New Zealand Institute of Forestry local sections. The response to this publicity was moderate and was scattered nationwide. As a result we decided to approach forest growers through several forest management consulting firms who work directly with small-plantation growers. In this manner we were able to assemble a dataset of plots across the study area. These data were extracted from a scattered estate of small to medium forest entities. In the interests of confidentiality the forest owner has requested that we do not include any information that might lead to the identification of this estate. These data were supplemented by a small network of plots from woodlot growers in the region and data from a set of national forest inventory plots (Figure 3) collected for the purposes of measuring forest carbon (LUCAS). The data collected in the plots varied considerably and this has implications for the types of analysis that can be implemented.

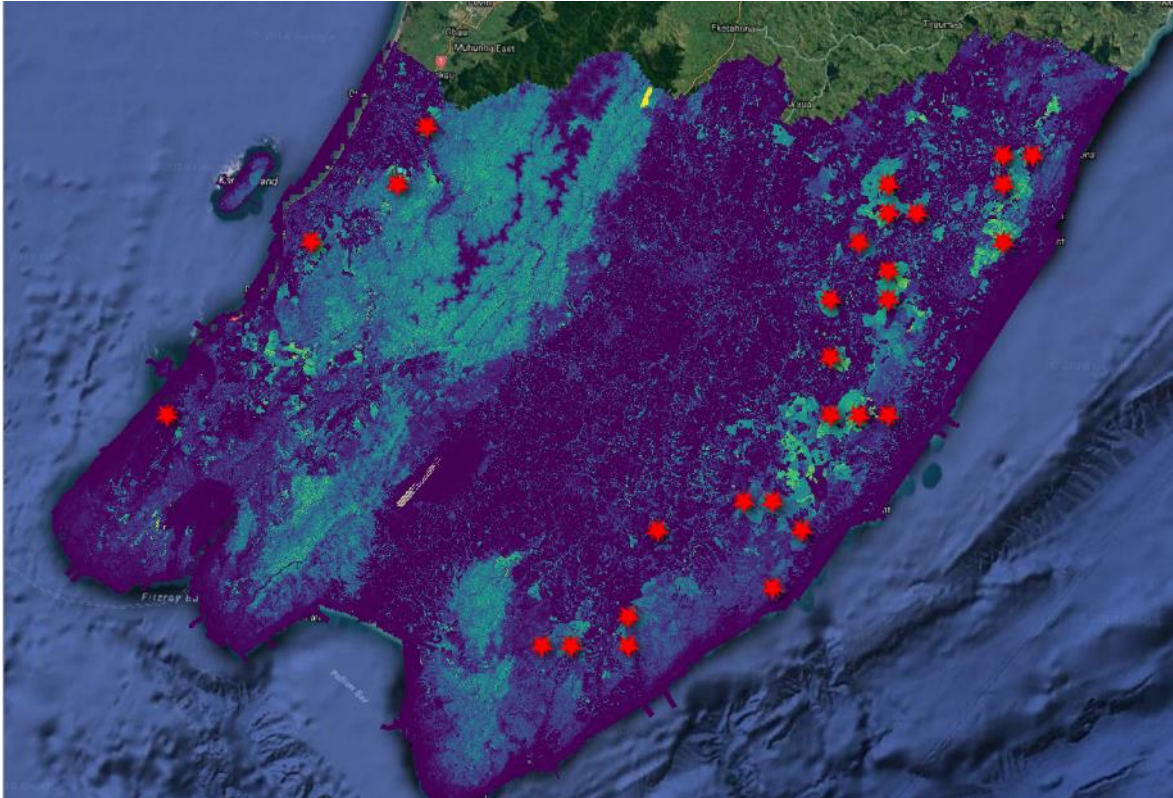


Figure 3. Location of the LUCAS plots (red stars) overlain on a raster showing the ALS metrics across the study area. The distribution shows that these plots represent good geographic coverage of the planted forest in the region.

ALS data and processing

The ALS data used in this project was collected on behalf of the Greater Wellington Council in 2014. An Optech ALTM 3100EA scanner was used for all surveys at a flying height of 1000 m AMGL. A scan frequency of 53 Hz was used at a pulse rate of 100 kHz with a scan angle restricted to 18 degrees. The swath width was 680 m and an overlap of 50 % ensured that the dataset was free from voids resulting in a density of 2.4 pls/m² and a last point spacing of 1.2 m. A series of ground control points (GCPs) were located in flat clear areas distributed throughout the study area. These were used to validate the vertical accuracy of the point cloud (RMSE = 0.095 m).

Initial data processing was carried out by the supplier in the Terrascan module of the Terrasolid software (Terrasolid, Espoo, Finland). This included flight line alignment, noise removal, and ground classification. Subsequent processing was carried out in the LAStools software (RapidLasso GmbH, Germany). Due to the very large size of the dataset we investigated methods based on cloud computing services. A high performance computing instance was established through Amazon Web Services (AWS). The AWS instance consisted of a Windows 10 operating system running on two virtual SSD storage devices of 1.5 TB each, 40 Intel Xeon cores, and 60 GB of RAM. To take advantage of this computing power a LAStools batch script was developed that provided end-to-end parallel processing. The processing batch script included tile buffering, triangulation of a digital terrain model (DTM), normalisation of point elevation to a height above the local terrain, and calculation of a comprehensive set of metrics on the forest canopy. Metrics calculated included height percentiles ($H_{05}, P_{10}, P_{20}, \dots, P_{99}$), descriptive statistics on return distribution (Mean height of returns, standard deviation, skew, kurtosis etc.) and metrics describing the distribution of intensity data recorded by the scanner. Rasters with a square 25 m pixel size were produced detailing the distribution of the ALS metrics across the entirety of 800,000 ha study area. Processing in this environment took 16 hours indicating the exceptionally promising potential for processing very large datasets in a clustered cloud computing environment. This approach is also very cost effective for many users as they don't need to carry the expense of buying high performing computing hardware. In cloud computing the user pays for the actual computing time and data storage used. Processing of the WRC dataset cost around \$1000 or under 0.01\$/ha

making it extremely appealing. The parallel batch processing script and further description of the compute environment are available upon request from the report authors.

Plot data summary

For the purposes of this research we acquired a field dataset from within the SNI region (Table 1). The dataset had several limitations and it should be noted that during a full scale implementation of this approach a much larger dataset would likely be available. The dataset used for this implementation is summarised below. The field data available for sampling had several limitations that may limit its effectiveness for use.

- The field data may not cover the full age range of the sampling population.
- The field data may not cover the full range of silvicultural conditions.
- The data has limited spatial accuracy.
- The full spatial range of the resource was not covered.

None of these limitations meant that the field data available was not useful.

Table 1. Summary of the plot numbers and inventory type of the dataset assembled for the case study.

Source	Inventory Type	N
-	PHI	368
-	FMA	38
LUCAS	Carbon	28

All available field plots were processed to provide plot level measures of several key forest variables, including Volume, Top Height, basal area, and stocking. The calculation used and a summary of the variables extracted are shown in Table 2.

Table 2. Summary of the key stand variables calculated for each plot in the reference dataset including the calculation used. Values shown include the mean and the standard deviation (SD)

Variable	Mean and SD	Calculation
Basal area (m ² ha ⁻¹)	64.5 (288.5)	The sum of the cross sectional area of all plot trees divided by the plot area.
Top Height (m)	32 (4.9)	The mean height of the 100 largest trees per hectare; where largest is defined by tree DBH
Volume (m ³ ha ⁻¹)	694 (263.3)	$Vol = TopHeight * BA * (0.942(H_1 - 1.4)^{1.161} + 0.317$
Stocking (sph)	390(163)	Number of trees per hectare with a presence at 1.4 m

Producing a Target Dataset

Performing a yield imputation requires accurate data describing the boundaries of a target woodlot and in a production implementation of this approach these could likely be provided by the forest growers. Several study participants provided spatial data showing their forest boundaries and these were used in this analysis. However, we needed to augment this dataset to expand the area covered by the yield estimates we produced. Fortunately there are now numerous forms of free, or very low cost, data that we can take advantage of to acquire this information. Although comprehensive mapping of woodlot boundaries is not yet available for New Zealand, research by Scion and its partners aims to provide this in the coming years and we can be confident that with suitable investment this will soon be available. The work of Xu et al (2017) provides a good framework for how boundary definitions can be acquired. Unfortunately the dataset produced by Xu et al (2017) was not available for use in this research and so we undertook a woodlot delineation exercise to provide an imputation dataset in addition to the stand boundaries provided by the study participants. Stand digitisation was carried out using combinations of free imagery from the Wellington Regional Council and from false colour images extracted from the European Space Agency's (ESA) Sentinel-2 satellite. We found this combination to be highly effective as the high spatial resolution of the regional council imagery enabled high precision mapping and the expanded spectral characteristics of the Sentinel-2 imagery made differentiation of plantations from indigenous forests or stands of different species straightforward. In this research we made use of manual digitisation of stands but it should be noted that automated delineation can provide highly

accurate stand delineation based on these image sources. The target dataset was comprised of both woodlots digitised as part of this study and geographical data provided by study participants (Figure 4).

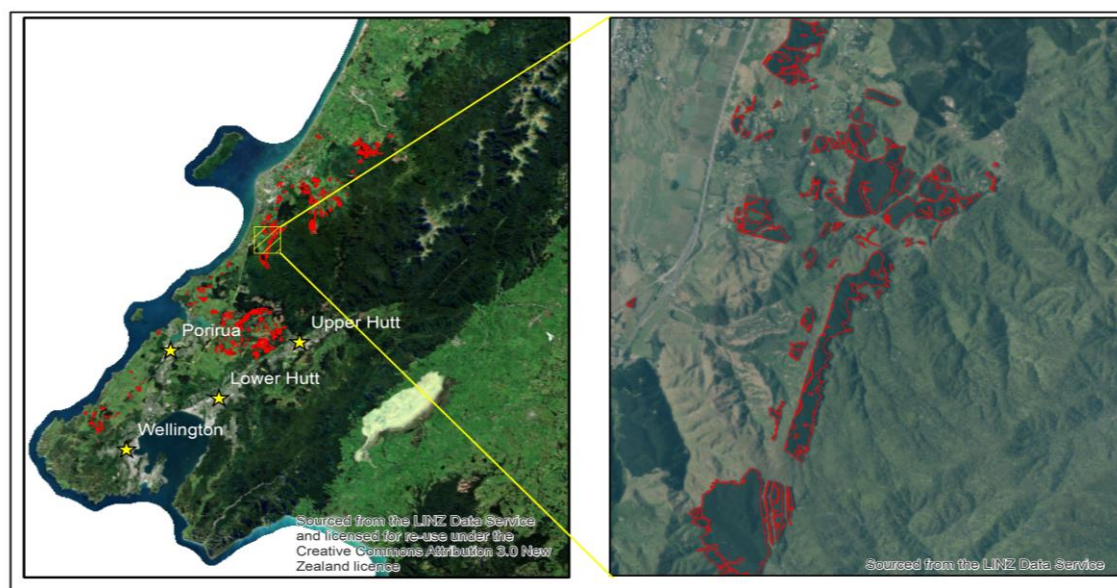


Figure 4. Examples of the digitisation process used to delineate woodlots and provide a target dataset for modelling efforts.

Yield imputation

A yield imputation was developed based on the reference dataset described earlier and descriptive metrics derived from the open access ALS point cloud that were concurrent with the ground measurement plots. No high grade positional information were available and so geo-locations provided by the forest grower were used. The accuracy of these locations was unknown and probably varied significantly. This is a source of error for this dataset but it is important that we understand whether data with a significant level of positional accuracy is still useful in this context. Recent research has shown that the lack of high grade positional accuracy in plot locations has a negligible effect on the precision of models produced when using ALS based forest inventory (McRoberts et al. 2017). Other authors (Jucker et al 2018) have suggested a method for overcoming positional inaccuracy based on the expected distribution of GPS points under canopy and these could be implemented in a full-scale application of this approach and may improve prediction accuracy.

Yield imputation procedures followed the well-established techniques used in New Zealand and Australia (Dash et al, 2015) and are summarised only briefly here for the reader's convenience. The general procedure developed in the R statistical programming language was:

- Generate ALS metrics across the entire study area.
- Spatially transform any ancillary data available for the forest and express this for each pixel across the area of interest. This along with the ALS metrics above finalised the target dataset where remotely sensed data is available but not field measurements.
- Process field measurements to provide plot level statistics
- Use the plot locations to extract ALS metrics for each plot and form a reference dataset.
- Use the reference data set to build a k-NN imputation model that can be used to assign reference plot observations to pixels in the target dataset based on the ALS metrics. This process requires that the analyst selects a set of predictor variables, a value for k, and a method of defining how similar the ALS data is between a reference and a target pixel. Some further information is given on this process below.
- Use the k-NN model to impute yields for the area of interest
- Summarise these yields according to boundaries that may be of interest.

There are several methods for quantifying the statistical distance between two observations that are available in the `yalp` package of R. The distance metric used defines the variant of k-NN model developed; each variant has its own strengths and weaknesses and several comprehensive reviews of these techniques are available. The most simple is Euclidean where distance is calculated as the Euclidean distance in normalised covariate space. A more complex approach, that has been shown to offer improved performance, is based on the random forests algorithm. Unlike imputations based on Euclidean distance the random forests metrics can use both categorical and numeric predictors. We used the random forest distance metric as it has been shown to provide superior performance in this forest type and for similar applications in the past.

During an imputation the analyst must select a means of defining the distance between two observations (How we define nearest neighbours), a value of k (how many neighbours are used for each target), and an appropriate method for weighting donor observations if $k > 1$. All these selections affect model behaviour and prediction quality and are the topics of much research effort. The random Forest algorithm (Breiman 2001) was used to define the distance in covariate space between target pixels and reference observations in this study. Using the random Forest distance matrix has been shown to have numerous favourable properties in an imputation context and has been successfully used to impute multivariate forest yields by numerous authors (Dash et al. 2015; Hudak et al. 2008). The analyst can either choose to set the value of k to 1 or to a larger value; in the latter case some sort of error minimisation procedure is frequently followed. In this study a value $k=1$ was selected as this has several advantages including simplicity in the modelling framework and yield processing, and maintenance of the variance structure in the reference dataset as larger k values tend to cause predictions drawn to the reference mean. The selection of k also means that the selection of a weighting regime for multiple donors to a given target is not required.

Based on these settings a k-NN model for the SNI was developed. The relationship between the predicted and observed values provides an indication of the model performance (Figure 5). This figure shows that there is a reasonable correspondence between observed and predicted values for volume and top height and that this is somewhat worse for basal area and stocking. The objective of this research is not to build the best possible k-NN model for yield prediction from ALS data as significant work has already provided guidance on this. Our objective is to test whether the data acquired for this project can be of use for imputing yields for small forest growers. As such we observe that the predictive power of the k-NN model is good enough to provide meaningful information and we subsequently proceeded to check whether we can use this in a practical manner.

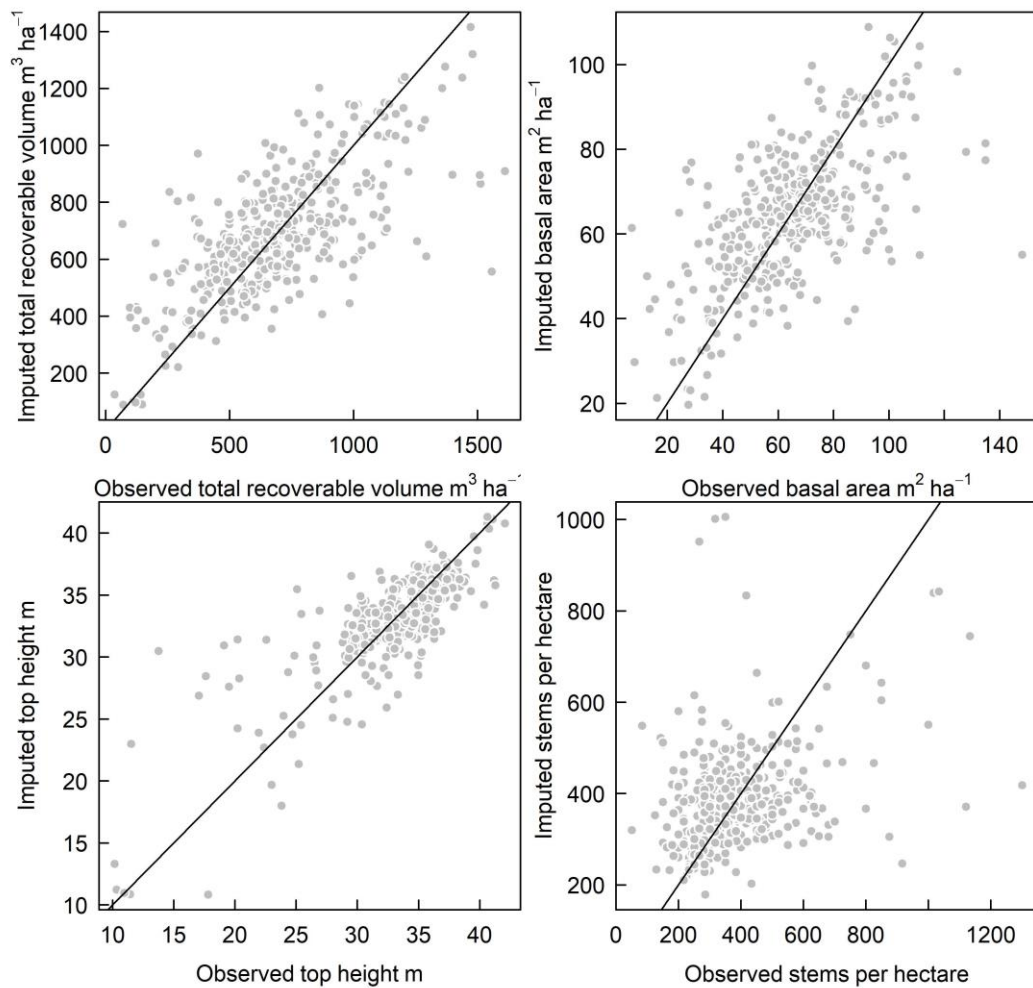


Figure 5. Results of the leave one out cross validation based on the fitting dataset using in the imputation for the SNI.

Model validation statistics (Table 3) show that model performance was good for top height, moderate for TSV and Basal area and only poor for Stocking. Model performance could easily be improved through more rigorous model tuning and incorporation of additional predictor variables into the model fitting dataset. This was beyond the scope of the current project as this project was simply intended as a proof of concept.

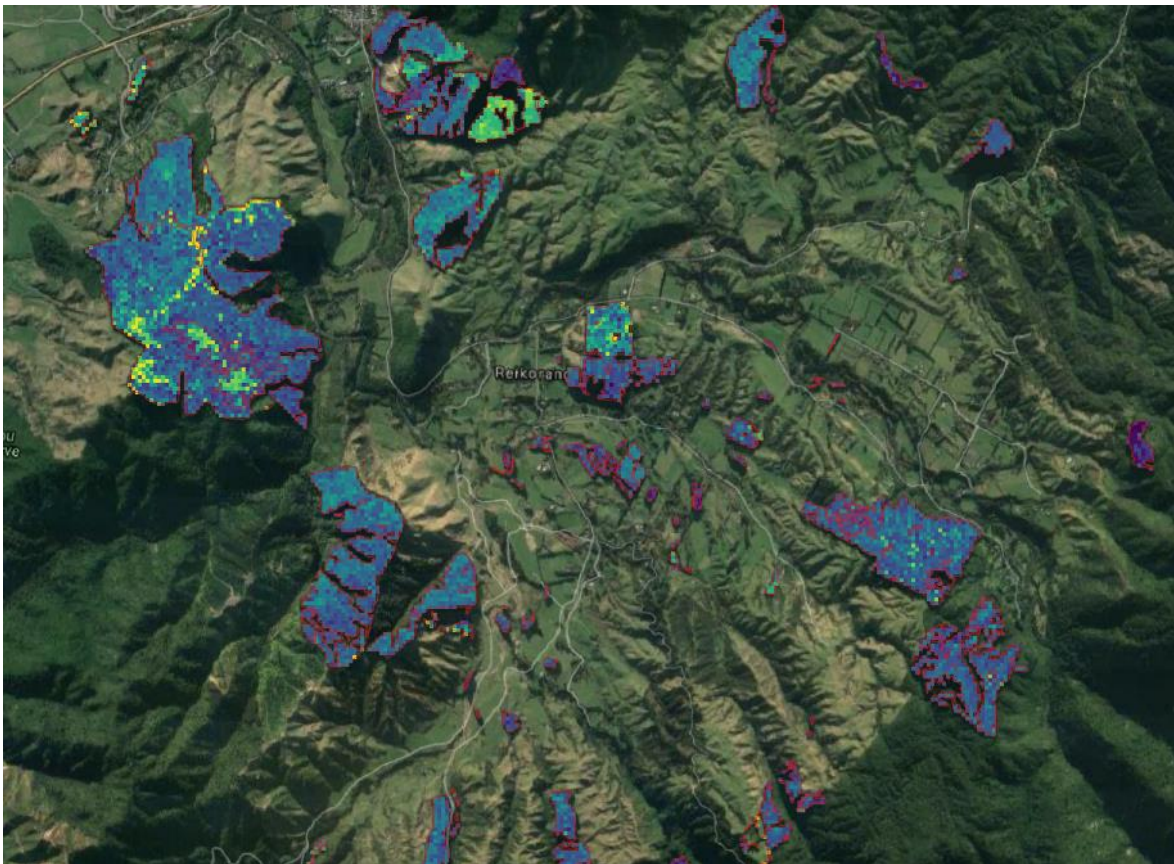
Table 3. Summary of model validation statistics. Values shown include relative root mean square error (RMSE) and mean absolute deviation (MAD)

Variable	RMSE %	MAD %
Total Standing Volume	28.2	20.1
Top Height	8.5	5.8
Basal Area	26.4	18.9
Stocking	42.1	28.2

Imputation of yields across study area

With the imputation model developed, the next task is to provide a valid means of imputing this over an area of interest. In the current study the area of interest was the target dataset specified above. Imputation is quite simplistic although special consideration is necessary where target pixels overlap stand boundaries. The approach taken for the imputation was to largely ignore the boundary issues. The Lidar metrics describing the forest canopy of boundary cells will be affected by the mix of stand types and land uses contained within. This approach may lead to some small errors around stand boundaries but these are insignificant compared to the advantages made through calculation simplicity when using this approach.

It should be noted that yields were generated for all delineated woodlots within the ALS coverage. This includes stands that had no field plots and is indicative of the capacity of this approach to provide potentially valuable yield data for stands belonging to participants with very few or no plots under a collaborative collective agreement.



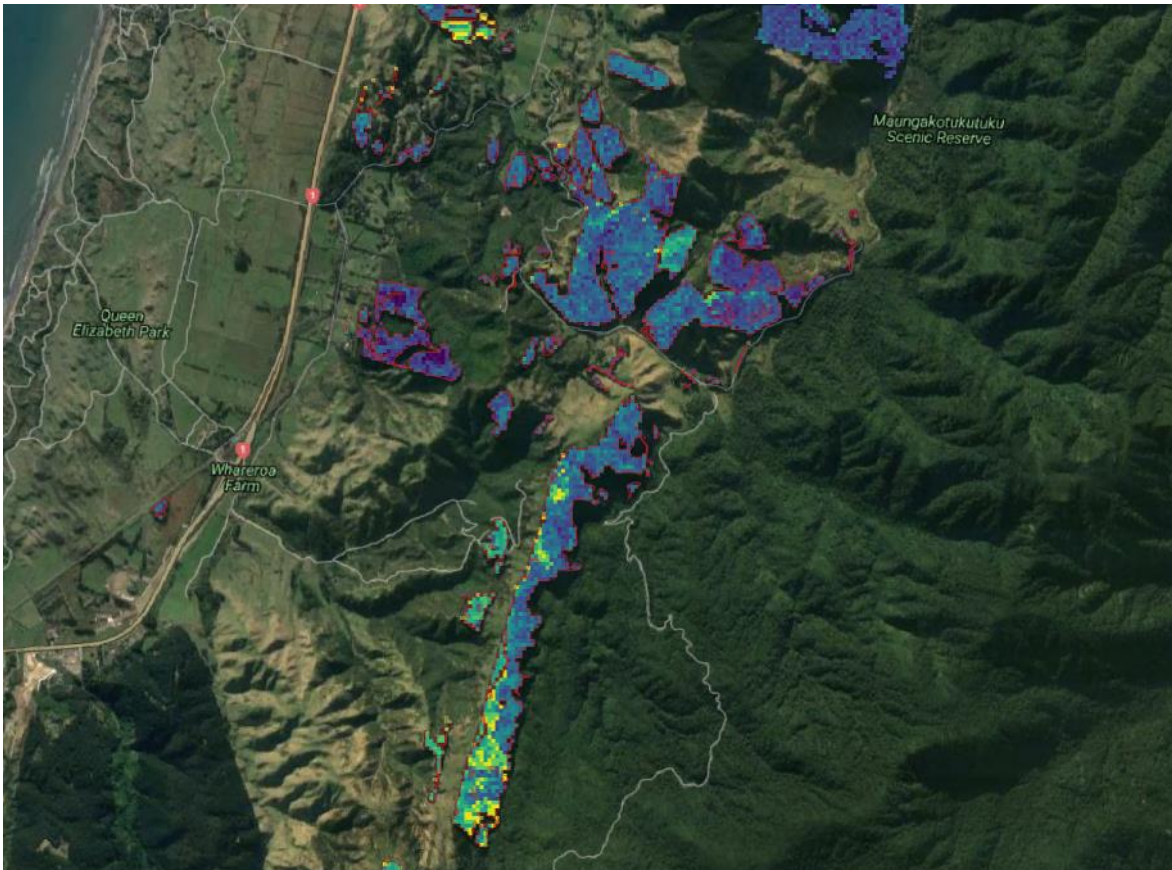


Figure 6. Examples of the spatial surfaces that result from the kNN imputation model based on the proof of concept case study detailed in this report.

In total, yields were estimated for 756 distinct small forests across the Wellington areas with a total area of 7,825 ha (Figure 6). The average size of forests in the study was 10.4 ha.

Independent Validation

A full validation of the quality of the prediction of the imputation model for all stands in the target dataset is beyond the scope of this study. However, a single forest scale dataset was left out of all model development to provide an independent dataset and to provide us with some understanding of the likely performance of the model when applied to new data. The subject forest (Mangaone North Forest) is a radiata pine woodlot (~150 ha) planted in 1992. In 2012 (two years prior to ALS survey) a detailed inventory of the forest was carried out to assess the forest yields and report on carbon sequestration. The plot measurements were grown to ALS survey date to provide a comparison. Using information provided by the forest grower the prototype calculation framework was used to predict yields at ALS survey date (Table 3). This comparison showed that the prototype calculations were reasonable for the Top Height and Volume variables but relatively poor for basal area and stocking. There was a substantial over prediction of volume but the errors were within the range suggested by the model validation statistics and would likely improve significantly with a larger fitting dataset and more advanced feature development and model tuning. This comparison suggests the prototype framework predictions are sufficiently accurate enough to be useful.

Table 3 Measured yields for Mangaone forest and the predictions outputted from the prototype calculation framework.

Variable	Measured	Predicted
Top Height	32.7	31.8
Volume	546.9	610
Basal Area	49.5	59.3
Stocking	262.7	360

Conclusion

In this case study we showed that it is possible for small-plantation growers to collaborate through data sharing and, where available, take advantage of open access datasets to provide yield estimates for small-plantations across an entire region. This can be done even for forests and woodlots where no plots have been measured. We have established a case study as a proof of concept of how this system might work in practice. Through disseminating these findings to relevant groups it is hoped that the potential for a collaborative approach amongst small-growers will become evident. Future work should focus on a full implementation of this type of approach in a region with a significant and motivated population of participants. From our experience it seems that the most convenient way to identify participant and access data would be through forest management consultants working in the region.

References

- Breiman, L. (2001). Random Forests. *Machine Learning*, 45(1), 5–32.
<https://doi.org/10.1023/A:1010933404324>
- Dash, J. P., Marshall, H. M., & Rawley, B. (2015). Methods for estimating multivariate stand yields and errors using k-NN and aerial laser scanning. *Forestry*, 88(2), 237–247.
<https://doi.org/10.1093/forestry/cpu054>
- Hudak, A. T., Crookston, N. L., Evans, J. S., Hall, D. E., & Falkowski, M. J. (2008). Nearest neighbor imputation of species-level, plot-scale forest structure attributes from LiDAR data. *Remote Sensing of Environment*, 112(5), 2232–2245.
<https://doi.org/10.1016/j.rse.2007.10.009>
- Jucker, T., Asner, G. P., Dalponte, M., Brodrick, P., Philipson, C. D., Vaughn, N., ... Coomes, D. A. (2018). Estimating aboveground carbon density and its uncertainty in Borneo's structurally complex tropical forests using airborne laser scanning. *Biogeosciences Discussions*, 2018, 1–29. <https://doi.org/10.5194/bg-2018-74>
- McRoberts, R. E., Chen, Q., Domke, G. M., Næsset, E., Gobakken, T., Chirici, G., & Mura, M. (2017). Optimizing nearest neighbour configurations for airborne laser scanning-assisted estimation of forest volume and biomass. *Forestry: An International Journal of Forest Research*, 90(1), 99–111. <https://doi.org/10.1093/forestry/cpw035>
- Xu, C., Morgenroth, J., & Manley, B. (2017). Mapping Net Stocked Plantation Area for Small-Scale Forests in New Zealand Using Integrated RapidEye and LiDAR Sensors. *Forests*, 8(12).
<https://doi.org/10.3390/f8120487>

Theme 3: Calibrating a National ALS model of Total Standing Volume using Local Sample Plots

Introduction

Forest inventory provides the information needed to manage production forests and to plan their harvest. Traditional inventory methods use field measurements to sample the forested area and produce estimates of total stem volume or, in more detail, potential log-product volume per hectare. To reduce costs and increase accuracy, remote sensing is now widely used, especially airborne laser scanning (lidar) which has been applied in forestry for over fifteen years (Næsset, 2014)

A significant proportion of New Zealand's radiata pine (*Pinus radiata* D. Don) estate is growing in small forests or woodlots. Pre-harvest inventory estimates are used to determine optimal time of harvest and may be the basis for the sale of the woodlot to timber processors or log exporters. It is difficult to measure such small stands in a cost-effective way as the number of plots required to produce estimates at the commonly accepted level of precision varies little whether the stand is five hectares or several hundred. Furthermore the proportion of the stand area which is close to the boundary increases rapidly with small stands, especially as woodlot boundaries may follow contours of small blocks deemed unsuitable as pastoral land. This makes the inventory more difficult as trees on the edge of a stand typically have over 10% more volume than those in the interior (Gordon and Pont, 2015) and so must be included proportionally in the sampling frame to avoid bias.

Data from a national inventory of the carbon stocks of New Zealand's radiata pine forests have been used to develop a national model to predict V from lidar metrics (Watt and Watt, 2013). This model is driven by two metrics: lidar mean height and the percentage of lidar ground returns, and accounted for 85% of the variance in V . Lidar mean height was most strongly related to V , and was incorporated in the model as a quadratic. Extensive testing with environmental and stand-level information showed little bias, indicating that this national-level model may provide a simple but robust method for deriving V from ALS data for all radiata pine sites and stand conditions.

Design-based approaches to using ALS supplemented by ground plots have been shown to be effective in improving the precision of estimated V . For example, a confidence interval approximately 2/3 smaller was derived for a 200ha forest by combining plot measurements with an ALS model of volume as a simple function of canopy height, compared with plot measurements alone (Corona and Fattorini, 2008). Calibration of national models has been examined in Finland on a large scale (Kotivuori et al., 2018), with decreases in root mean square errors of 2 to 3% when applied at a regional level. Different ALS campaigns will typically use different acquisition parameters leading to concern that lidar metrics may differ by campaign (Rombouts et al., 2008), although there is evidence that the relationship between lidar metrics and field data remain valid across time (Fekety et al., 2014). It appears that height metrics, especially dominant height, are not affected greatly by variations in different ALS data sets and can be accurately predicted without corresponding field measurements (Kotivuori et al., 2016; Gopalakrishnan et al., 2015). If differences do exist then calibrating the model estimates via ground plots will effectively account for them.

This case study was designed to test the efficacy of the national ALS model (Watt and Watt, 2013) when applied to ten stands of radiata pine in New Zealand's Central North Island. In particular we examined the accuracy of estimates derived by combining local samples (16 plots) gathered from ground-based measurement with wall-to-wall estimates of V derived by applying the national model to ALS data captured via UAV, and compared these with the un-calibrated ALS model and estimates from high-intensity ground plots.

Methods

Study sites

The forest sites are located in the Central North Island of New Zealand located at altitudes from 400 to 700 masl. Ten stands were available to the study ranging in size from 20 to 120 hectares. A variety of adjoining land-use was evident, from pasture, indigenous forest and further stands of radiata pine. Productivity extended to over 30 m³ ha⁻¹ annum⁻¹.

Field data

All stands had been field-measured using circular, bounded, slope-corrected sample plots of 0.06 ha at a rate of around one plot per two hectares. The plots were located systematically on arbitrary grids to ensure spatial coverage of each stand. For example, in stand H11 thirty sample plots were located on a regular grid, although several grid-points were ruled out as falling in exclusions (internal mapped-out non-stocked areas). Plot centres were located using a Trimble Geo7X GNSS (Trimble Ltd., Colorado, USA) and differentially corrected using a series of local base stations maintained by Land Information New Zealand (LINZ). The over-bark diameter at breast height (DBH measured at 1.4 m) of all radiata pine trees within the plot was measured. Tree height was measured on a sample of plot trees spanning the diameter distribution within each plot that were free from excessive lean or malformation. The sample plots were processed using a compatible polynomial volume and taper equation (Gordon, 1983; Goulding and Murray, 1976) using coefficients derived from destructive tree taper studies in the same geographical region to provide estimates of standing tree volume. Stem profiles were then exposed to an optimal log bucking algorithm in a commercial forest yield prediction software package (YTGEN, Silmetra, Tokoroa, New Zealand) to provide estimates of total recoverable volume (*TRV*) and log product volume estimates. These volumes were summed within each plot and adjusted for plot area to determine total stem volume on a per-hectare basis, (V m³ ha⁻¹).

Airborne Laser Scanning Data

For stand H11 the ALS data were acquired using a Velodyne 32 HDLe (Velodyne, San Jose, USA) scanner embedded in LidarUSA Snoopy A-Series laser scanning system (LiDARUSA, Alabama, USA). The laser scanner was mounted to an Altus ORC4 remotely piloted helicopter platform (Altus Ltd., Hamilton, New Zealand). A flying altitude of around 80 m above the local terrain was used and the flight plan ensured that there was significant side overlap to remove the possibility of data voids and all flight manoeuvres and altitude adjustments were made outside of the area of interest to avoid the possibility of flight artefacts in the dataset. The laser scanner is only capable of recording a single return but the resultant had a pulse density of 712 pls m² and a pulse spacing of 0.04 m. Flight line matching, ground classification, noise removal, and identification of overlap point was carried out in the Terrasolid software (Terrasolid Oy, Espoo, Finland). Subsequently overlap points were removed to ensure a more even density over the entire study area and descriptive metrics were calculated for the area of interest using the LidR R package. Metrics were calculated at a 25 m resolution and included those used in the national *V* model (Watt and Watt 2013) describing the maximum height of returns within a grid cell (H_{max}), the mean height of returns (H_{mean}), and the percentage of all returns that reached the ground (P_{zero}).

For all remaining stand an airborne laser scanning (ALS) dataset was made available by the forest manager of Lake Taupo and Lake Rotoaira forest. Data collection and cleansing took place between the 30/05/2017 – 1/02/2018 2018 using a fixed wing aircraft at a capture altitude of 700 magl using a Riegl Q1560 scanner. Flight planning ensured a between swath overlap of 55 % to ensure the dataset was free from voids. A pulse repetition frequency of 360 Khz was used and the scanner collected multiple returns per pulse. The resulting point density was 4.79 pts/m². Initial pre-processing was completed by the supplier using the Terrasolid software. This included flight line matching, ground classification, and noise removal. Subsequent point cloud processing was carried out in the LAStools software. The ground classified points were used to produce a digital terrain model (DTM) for the study forest. This was used to normalise elevations of the non-ground returns and to describe the terrain features of all plots. The normalised point cloud was used to provide auxiliary data on the study population. Rasters detailing descriptive metrics calculated from the point cloud at a 25 m spatial resolution were generated using the LAScanopy tool in the LAStools software. Metrics calculated included height percentiles (H_{05} , P_{10} , P_{20} , ... P_{99}), descriptive statistics on return distribution (Mean height of returns, standard deviation, skew, kurtosis etc.) and metrics describing the distribution of intensity data recorded by the scanner

Analysis

The sets of field plots were treated as simple random samples (SRS) to calculate the mean and variance of V for each stand. Using this variance and the plot size and stand area, the precision of these estimates were calculated. Precision was expressed as Probable Limits of Error (PLE), a relative measure defined as half the ninety-five percent confidence interval as a percentage of the estimated mean.

To obtain an un-calibrated estimate from the lidar coverage of each stand via the national model, the stand boundaries were intersected with the lidar raster and V_{lidar} calculated for each cell using the lidar metrics H_{mean} and P_{zero} following Watt and Watt's (2013) national ALS model. Because of the sensitivity of V_{lidar} in cells close to the stand boundaries, only those cells wholly within the stand were used to contribute to these wall-to-wall calculations of the population mean V_{lidar} . These un-calibrated estimates from the national model were compared with field plot means of V and used as the basis for calibrated estimates.

Regression Estimation was then used to calibrate the national ALS model using sub-sets of the local plot data. Regression Estimation is a widely applicable method (Robinson, 2011) which requires an approximate linear relationship between the ancillary variable (V_{lidar}) and the target variable (V) to estimate the target variable mean (Equation 1), as,

$$\bar{V}_R = \bar{V} + b(\mu_{V_{lidar}} - \bar{V}_{lidar}) \quad (1)$$

The method uses the difference between the population mean of V_{lidar} and the mean of the V_{lidar} associated with the sample of calibration plots, to adjust the mean V from the calibration plots. The population mean of V_{lidar} must be known. The rate of adjustment (b , the regression coefficient) ensures the estimate is un-biased. The standard error of V_R is a function of the variance about the regression line, the distance of the sample ancillary mean from the V_{lidar} population mean, the sample size and finite population correction (Robinson, 2011). The relationships between V and V_{lidar} were examined to verify that the assumptions of regression estimation (linear relationship, homogeneous variance) were not violated. Regression sampling is classified as a model-assisted estimator by Ståhl *et al* (2016).

To obtain long-run averages of the efficacy of regression estimation a simulation procedure was used. For each stand in the study, a sample of plots was simulated by over-laying a grid with random origin and orientation over the stand which made sixteen intersections within the polygons describing the stand boundary. The nearest existing ground plots to the intersections were selected and used to calculate both a regression estimate (V_R , Equation 1) and a SRS estimate. The estimates and their PLE and reliability were recorded. This procedure was repeated 10000 times for each stand. The data generated by the simulation runs were compared for each stand with the mean V from all plots and summarized as root mean square errors (RMSE), mean differences (MD), the distribution of PLE and the reliability.

This procedure simulates random grid-based sampling. Grid-based sampling has been shown to be one of the most effective ways of covering spatial variation in the absence of prior information to guide sample locations (Gordon and Pont, 2015; Maltamo, 2011; Morrison *et al*, 2008). The "reliability" of the estimate of the mean was calculated as the proportion of simulations in which the calculated confidence interval contained the all-plot mean. This statistic is only useful to compare the SRS and calibrated national model results, since it is based on the same set of plots from which the sixteen-plot samples were drawn.

Results

The intersection of the raster with the stand boundary was examined by calculating the proportion of each raster cell that was included within the stand boundary and relating this to V_{lidar} for stand H11 (Figure 1).

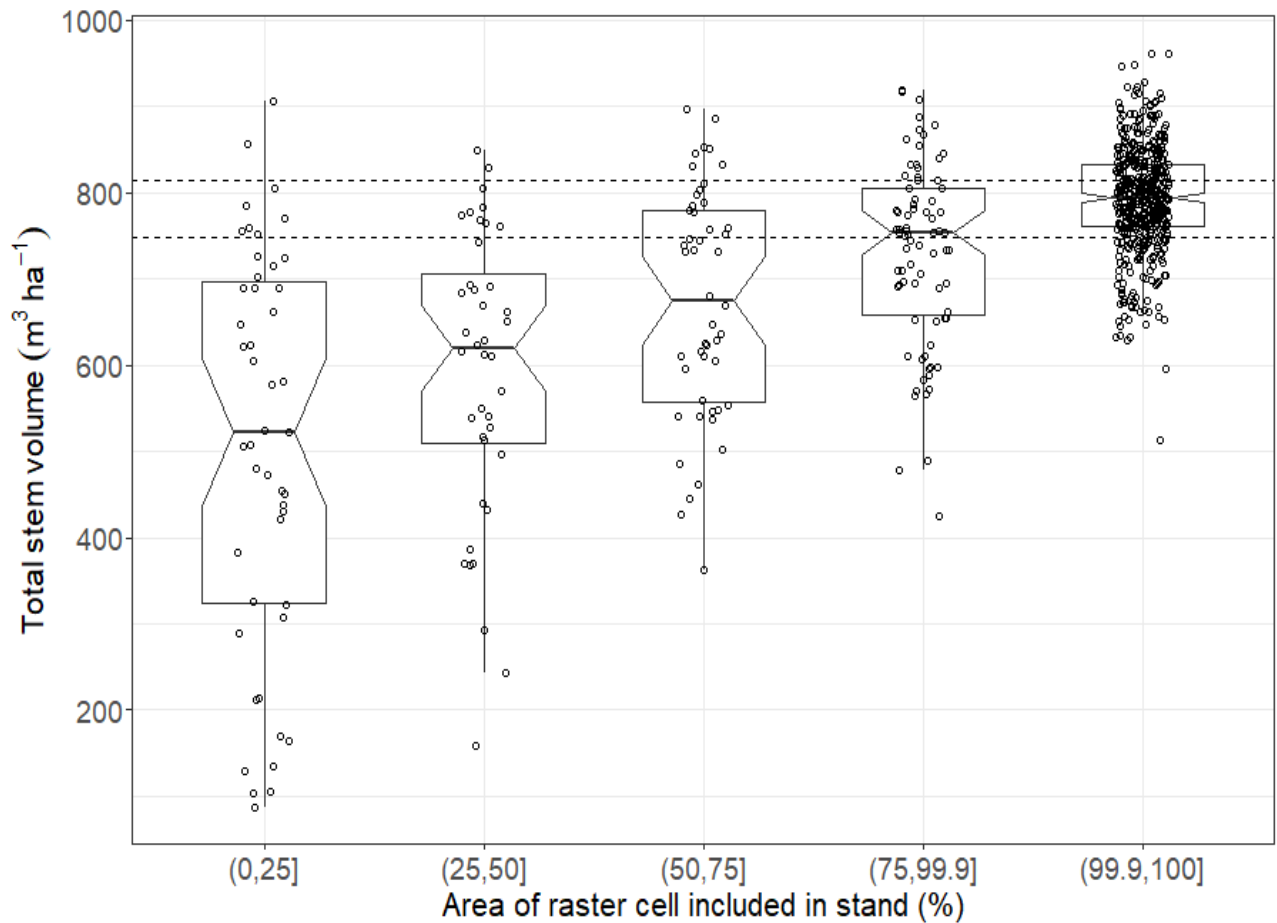


Figure 1: Comparison of V_{lidar} distributions by percentage of raster cell area included in stand H11. The boxes are notched at the median and range from the first to the third quartile. Whiskers extend to extreme values no more than 1.5 times the inter-quartile range beyond the box. Boxes with notches that do not overlap are likely to have significantly different medians. Horizontal dashed lines illustrate the 95% confidence interval around the plot mean V .

All subsequent analyses used only those raster cells wholly contained within the stand boundaries.

The initial comparison looked at the un-calibrated national model estimates of total standing volume (V). Figure 2 shows differences between the model estimates and plot estimates, related to the lidar mean height metric for each of the ten stands. The difference in the V values is expressed as a percentage of the national model estimate. About half the estimates are within $\pm 5\%$ of the zero line with the rest extending to nearly 80% under-estimate. The under-estimates appear to be related to the size of the lidar metric with greater underestimation occurring at lower values of lidar mean height.

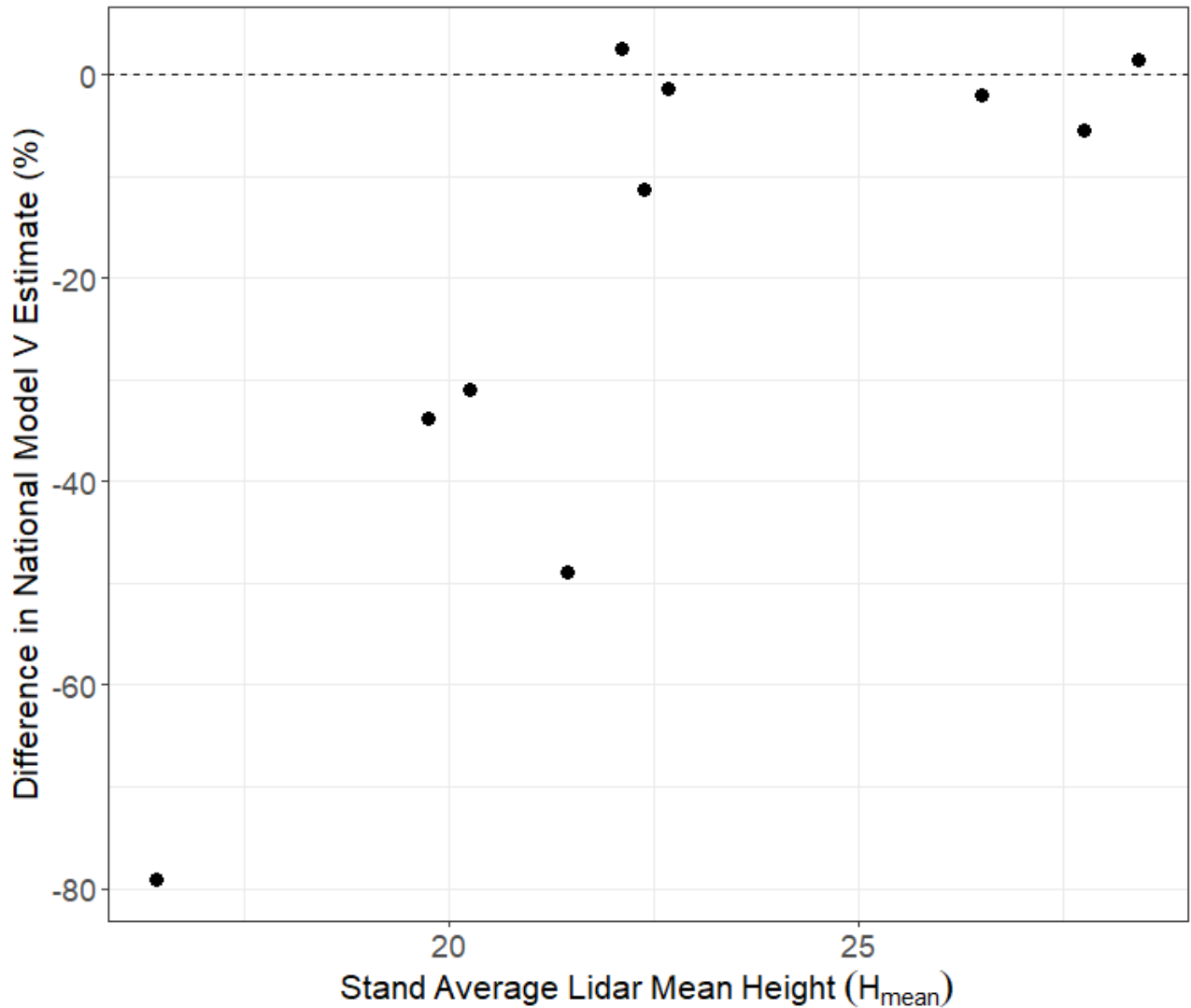


Figure 2: Difference between the un-calibrated national model estimates and the plot-based mean V , related to the lidar metric H_{mean} , averaged over the raster. The difference is expressed as a percentage of the National Model estimate.

Simulations

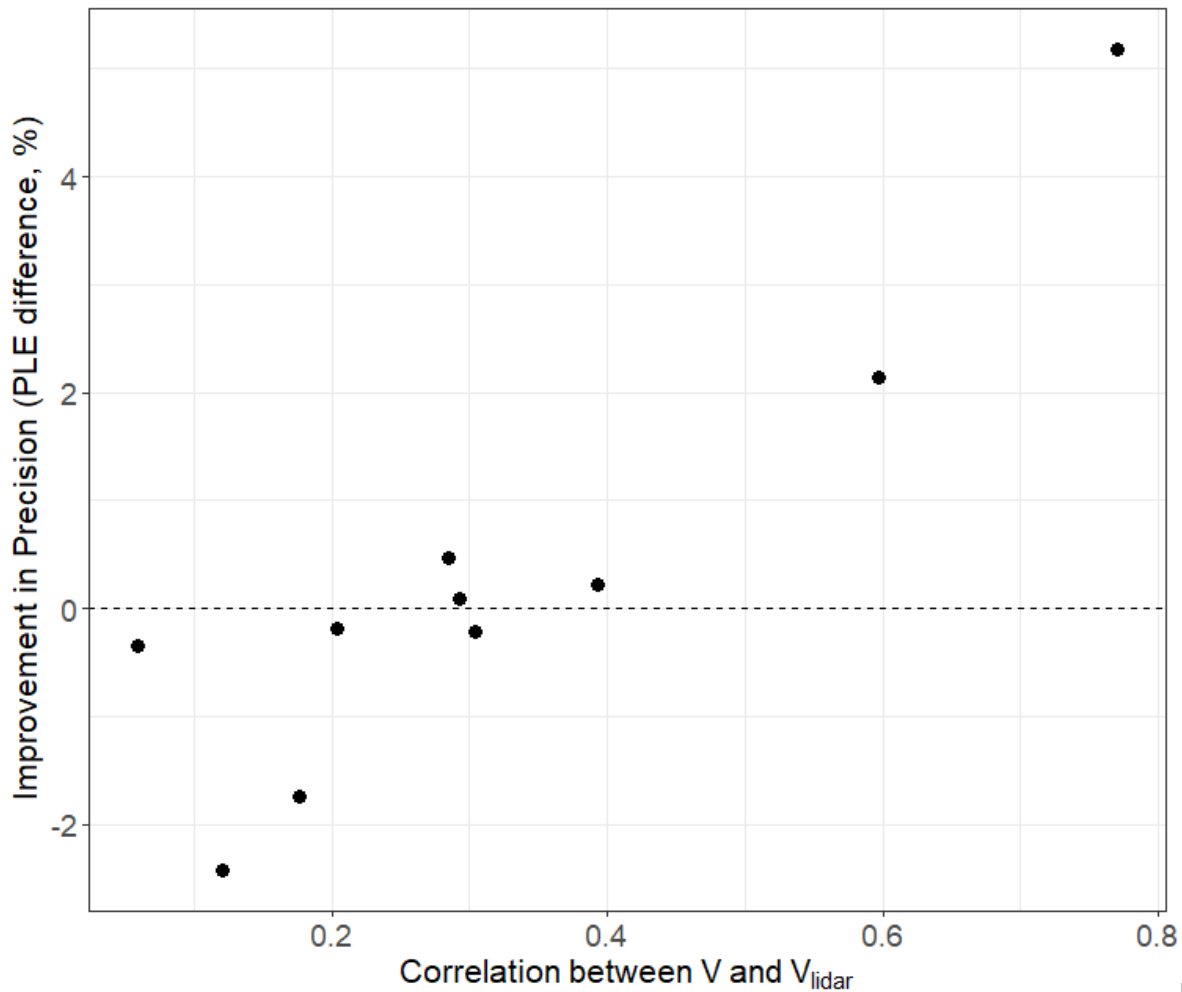
The V_{lidar} population mean of each stand was used as the calibration point at which the regression between the plot V and the ancillary variable, the associated cell V_{lidar} , was used to produce an estimate of V_R in each simulation run (Equation 1).

The results of the simulations for 16 calibration plots are shown in Table 1. Each simulation was repeated 10000 times to ensure stable averages.

Table 1. Simulation Results using 16 calibration plots. RMSE is the root mean squared error ($\text{m}^3 \text{ha}^{-1}$). MD is the mean difference ($\text{m}^3 \text{ha}^{-1}$).

Stand	Simple Random Sample (SRS)				Calibrated National Model (CNM)			
	RMSE	MD	PLE %	Reliability %	RMSE	MD	PLE %	Reliability %
R6801	27.4	-9.3	12.4	98.2	27.8	-1.0	14.8	99.1
R7701	33.0	-4.4	15.2	99.6	39.2	-14.3	17.0	99.4
R7601	34.0	-0.8	15.1	99.0	36.0	1.4	15.4	98.7
L8206	24.8	9.4	8.0	97.3	25.2	17.2	8.2	97.5
R118011	35.6	25.0	11.5	96.9	36.8	28.3	11.7	97.3
L29011	21.2	1.7	16.6	100.0	22.0	-0.1	16.5	100.0
H11	17.2	3.6	5.5	98.9	15.5	1.6	5.3	99.4
L8903	26.6	-5.8	10.1	99.0	26.2	-2.1	9.7	98.6
R7801	32.8	3.2	14.2	99.1	33.8	-19.2	12.1	94.7
L17502	53.3	44.9	18.5	97.4	48.9	44.3	13.4	96.9

Only one large improvement in precision are seen was observed through use of the calibrated national model over a SRS of the calibration plots (R6801). This appears to be from the stand with the highest variation in V which had the highest correlation between V and the associated cell V_{lidar} . The difference in average PLE by stand is shown in Figure 3 in relation to the correlation between V and the associated cell V_{lidar} .



Figure

3: Improvement in precision through using the calibrated National Model in relation to the correlation between calibration plot V and the associated cell V_{lidar} .

Discussion

Without calibration, the national model estimated the mean total stem volume to within $\pm 5\%$ of the plot-based estimates for five stands. The estimates for the remaining stands were all considerably below the plot-based estimates. This suggests that for pure, even-aged plantations of *P. radiata* in New Zealand the national model is transferable in some cases. The under-estimates appear to be related to the size of the H_{mean} lidar metric but their magnitude is in keeping with the variation illustrated in Watt and Watt (2013) Figure 3, which shows V ranging from 200 to 700 at an H_{mean} value of 20m.

The reduction in estimated total stem volume (V_{lidar}) with decreasing intersection between the raster cell and the stand (Figure 1) was a result of the reduction in the lidar metric H_{mean} , probably due to this stand (H11) being bounded on three sides by pasture or road-edge. Limiting the raster to those cells wholly within the stand resulted in a consistent population of V_{lidar} values, compatible with the plot-based V .

However none of the 30 plots in H11 sampled the stand edge, which can be a significant proportion of small, woodlots, and which typically contains slightly higher V than the stand interior. Reducing the pixel size may help with edge-effects (for example, Corona and Fattorini (2008) used 1 m² pixels), but it is possible that the lidar metrics used by the national model would become too noisy unless smoothed using spatial interpolation.

The simulation results showed that using 16 plots to calibrate the national model produced a variety of results in term of precision relative to a SRS of these plots. Results show that unless there is a strong correlation or a larger sample, little information can be extracted from V_{lidar} as an ancillary variable. Little gain from calibration has also been noted by Kotivuori et al (2016) with respect to estimating stand height, where their nationwide model performed well without calibration.

As the national model used here is primarily a function of height there is perhaps some agreement with the Finish results.

It is possible that better registration between the plot location and the section of the lidar point cloud used to derive the associated metrics could improve the correlation between V and V_{lidar} . If the error in GPS plot location could be reduced, a custom cylinder of the point cloud could be extracted to derive H_{mean} specifically for each calibration plot.

The small size and isolated nature of radiata pine woodlots make them difficult targets for traditional inventory procedures. Costs should be kept commensurate with the value of the resource but the estimates must be accurate enough to support confident harvest planning and sales agreements. More work is needed to examine the accuracy of the un-calibrated national model and identify where and why the estimates are poor. This should focus on pre-harvest inventory and attempt to span the range of site productivity and final crop stocking seen in radiata pine woodlots.

References

- Corona, P., & Fattorini, L. (2008). Area-based lidar-assisted estimation of forest standing volume. *Canadian Journal of Forest Research*, 38(11), 2911-2916.
- Fekety, P. A., Falkowski, M. J., & Hudak, A. T. (2014). Temporal transferability of LiDAR-based imputation of forest inventory attributes. *Canadian Journal of Forest Research*, 45(4), 422-435.
- Gopalakrishnan, R., Thomas, V. A., Coulston, J. W., & Wynne, R. H. (2015). Prediction of canopy heights over a large region using heterogeneous lidar datasets: efficacy and challenges. *Remote Sensing*, 7(9), 11036-11060.
- Gordon, A. Comparison of Compatible Polynomial Taper Equations. *New Zealand Journal of Forestry Science*, 1983, 13, 146–155.217
- Gordon, A. D., & Pont, D. (2015). Inventory estimates of stem volume using nine sampling methods in thinned *Pinus radiata* stands, New Zealand. *New Zealand Journal of Forestry Science*, 45(1), 8.
- Goulding, C.J., Murray, J.C. (1976) Polynomial taper equations that are compatible with tree volume equations. *New Zealand Journal of Forestry Science* 5, 313–322.
- Kotivuori, E., Korhonen, L. & Packalen, P. (2016) Nationwide airborne laser scanning based models for volume, biomass and dominant height in Finland. *Silva Fennica* 50, no. 4.
- Kotivuori, E., Maltamo, M., Korhonen, L., & Packalen, P. (2018). Calibration of nationwide airborne laser scanning based stem volume models. *Remote Sensing of Environment*, 210, 179-192.
- Maltamo, M., Bollandsås, O.M., Næsset, E., Gobakken, T., & Packalén, P. (2011) Different plot selection strategies for field training data in ALS-assisted forest inventory. *Forestry: An International Journal of Forest Research*, 84, 23–31
- Morrison, L., Smith, D., Young, C.W., & Nichols, D. (2008) Evaluating sampling designs by computer simulation: A case study with the Missouri bladderpod. *Population Ecology* (2008) 50: 417. <https://doi.org/10.1007/s10144-008-0100-x>
- Næsset, E. (2014). Area-based inventory in Norway—from innovation to an operational reality. In *Forestry applications of airborne laser scanning* (pp. 215-240). Springer, Dordrecht.
- Robinson, A.P., & Hamann, J.D. *Regression Estimation. In Forest Analytics with R*; Gentleman, R.; Hornik, K.; Parmigiani, G., Eds.; Springer: New York, USA, 2011; pp. 104–113.221
- Rombouts, J., Ferguson, I. S., & Leech, J. W. (2008). Variability of LiDAR volume prediction models for productivity assessment of radiata pine plantations in South Australia. In *Proceedings of SilviLaser 2008, 8th international conference on LiDAR applications in forest assessment and inventory, Heriot-Watt University, Edinburgh, UK, 17-19 September, 2008* (pp. 39-49). SilviLaser 2008 Organizing Committee.
- Ståhl, G., Saarela, S., Schnell, S., Holm, S., Breidenbach, J., Healey, S.P., Patterson, P.L., Magnussen, S., Næsset, E., McRoberts, R.E., & Gregoire, T.G. (2016). Use of models in large-area forest surveys: comparing model-assisted, model-based and hybrid estimation. *Forest Ecosystems* 2016, 3:5.
- Watt, P., & Watt, M. S. (2013). Development of a national model of *Pinus radiata* stand volume from LiDAR metrics for New Zealand. *International journal of remote sensing*, 34(16), 5892-5904.

Recommendations and Conclusions

Theme 1 tested different sampling strategies for forest inventories using UAV laser scanning and photogrammetric data. Results within this theme support the use of model-based estimation that incorporates wall to wall coverage of remotely sensed data, for improving inventory precision in small woodlots. Significant gains in relative efficiency, over use of only plot data, were achieved using this method. In contrast, gains in relative efficiency using partial-coverage auxiliary data were modest and this method should only be considered an option for rather large areas where reducing the auxiliary area coverage translates into a significant reduction in the time required for UAV operations. The results highlight the utility of photogrammetric point clouds collected from UAV (UAV-SfM_{DTM}) as a source of auxiliary data. The use of UAV-SfM_{DTM} data yielded some of the most precise estimates out of the studied data sources and variables of interest, highlighting the relevance of using UAV photogrammetric data for estimation of key variables such as stand density, basal area and total stem volume. Further research should examine the efficiency of model based estimation using UAV-SfM_{DTM} data for small woodlots that are established across a wide range in site conditions and cover a range in area.

Theme 2 investigated the potential benefits to small plantation growers that may result from data sharing. We showed that it is possible for small-plantation growers to collaborate through data sharing and, where available, take advantage of open access datasets to provide yield estimates for small-plantations across an entire region. This can be done even for forests and woodlots where no plots have been measured. We have established a case study as a proof of concept of how this system might work in practice. Through disseminating these findings to relevant groups it is hoped that the potential for a collaborative approach amongst small-growers will become evident. Future work should focus on a full implementation of this type of approach in a region with a significant and motivated population of participants. From our experience it seems that the most convenient way to identify participant and access data would be through forest management consultants working in the region.

Theme 3 investigated the feasibility of utilising a national LiDAR based model to predict total stem volume within 10 small woodlots. This was undertaken either through (i) uncalibrated direct prediction of volume using the LiDAR model and (ii) integration of calibrated predictions with plot data using regression estimation. Without calibration, the national model estimated the mean total stem volume to within $\pm 5\%$ of the plot-based estimates for five stands but considerably underpredicted total stem volume for the other five stands. This under-prediction was associated with stands that had lower mean heights estimated by the LiDAR. Although the use of calibrated predictions reduced the probable limit of error (PLE) for five stands, PLE was higher when only plots were used for the other five stands. Results clearly show that unless there is a strong correlation between predictions from the LiDAR based model and measured volume at the stand level, gains through use of this method are likely to be limited. More work is needed to examine the accuracy of the un-calibrated national model and identify why the estimates are poor under some circumstances. This should focus on pre-harvest inventory and attempt to span the range of site productivity and final crop stocking within small radiata pine woodlots.

Related articles and communications associated with this project.

Tree grower article

Dash, J.P., and Watt, M.S., 2017. Improving small-plantation and woodlot inventory using remote sensing... How can you help? Tree Grower 38 (2).

Article written and published in Friday Offcuts

<https://foresttech.events/improving-small-plantation-and-woodlot-inventories/>

Youtube video on the project

<https://www.youtube.com/watch?v=9REd2GhTqsw&t=19s>

Coverage in Scion's Connections

<http://www.scionresearch.com/about-us/about-scion/corporate-publications/scion-connections/past-issues-list/scion-connections-issue-26,-december-2017/new-ways-to-measure-and-value-small-forests>

Forest Growers Research Conference, Christchurch 2017 Presentation

<https://fgr.nz/documents/improving-small-plantation-woodlot-inventory/>

Acknowledgements

The authors acknowledge The Forest Growers Levy Trust, New Zealand Farm Forestry Association, AgMardt, The Neil Barr Foundation and Scion Strategic Science Investment Fund for providing financial support for this project. The project technical steering team of David Crawley, Paul Silcox, and Patrick Milne are recognised for their valuable contribution towards this research. The authors would like to acknowledge the forest Manager Jeff Tombleson for providing access to the study forest used in Theme 1 and for supporting our research. Ben Morrow and Robin Hartley of Scion are acknowledged for their contribution to UAV data collection for Theme 1.